Temporal distribution and diversity of cold-water corals in the southwest Indian Ocean over the past 25,000 years

Naomi Pratt[1], Tianyu Chen[2,3], Tao Li[2,3], David J. Wilson[1,4], Tina van de Flierdt[1], Susan H. Little[1], Michelle L. Taylor[5], Laura F. Robinson[2], Alex D. Rogers[6,7], Nadiezhda Santodomingo[8]

1. Department of Earth Science and Engineering, Imperial College London, South Kensington Campus, Exhibition Road, London SW7 2AZ, UK
2. School of Earth Sciences, University of Bristol, BS8 1RJ, UK
3. School of Earth Sciences and Engineering, Nanjing University, Nanjing 210023, China
4. Department of Earth Sciences, University College London, WC1E 6BS, UK
5. School of Biological Sciences, University of Essex, Wivenhoe Park, Colchester, CO4 3SQ, UK
6. Department of Zoology, University of Oxford, Tinbergen Building, South Parks Road, Oxford OX1 3PS, UK
7. Present address: REV Ocean, Oksenøyveien 10, NO-1366 Lysaker, Norway
8. Natural History Museum, Department of Earth Sciences, Cromwell Road, SW7 5BD, London, UK

Abstract

Fossil cold-water corals can be used to reconstruct physical, chemical, and biological changes in the ocean because their skeleton often preserves ambient seawater signatures. Furthermore, patterns in the geographic and temporal extent of cold-water corals have changed through time in response to environmental conditions. Here we present taxonomic and dating results from a new collection of subfossil cold-water corals recovered from seamounts of the

Southwest Indian Ocean Ridge. The area is a dynamic hydrographic region characterised by eastward flow of the Agulhas Return Current and the northernmost fronts of the Antarctic Circumpolar Current. In total, 122 solitary scleractinian corals and 27 samples of colonial scleractinian material were collected from water depths between 172 and 1395 m, corresponding to subtropical waters, Antarctic Intermediate Water (AAIW), and Upper Circumpolar Deep Water (UCDW). Fifteen species were identified, including eight species new to the region. The assemblage reflects the position of the seamounts in a transition zone between Indo-Pacific and Subantarctic biogeographic zones. Morphological variation in caryophyllids and the restriction of dendrophylliids to the southern seamounts could result from genetic isolation or reflect environmental conditions. Uranium-series dating using both rapid laser ablation and precise isotope dilution methods reveals their temporal distribution from the Last Glacial Maximum to the present day. Only one specimen of glacial age was found, while peaks in abundance occur around Heinrich Stadial 1 and the Younger Dryas, times at which ocean chemistry and food supply were likely to have presented optimal conditions for cold-water corals. A widespread regional preference of cold-water corals for UCDW over AAIW depths during the deglacial, the reverse of the modern situation, could be explained by higher dissolved oxygen concentrations and a temperature inversion that persisted into the early Holocene.

1. Introduction

1.1 Cold-water corals

Cold-water corals (henceforth CWCs) comprise non-symbiotic (azooxanthellate) cnidarian species of the orders Scleractinia, Octocorallia, Stylasteridae, and Antipatharia (Roberts et al., 2009). About half of all species of scleractinian corals are azooxanthellate, some of which can build structural habitats that provide refuge for many other species, although the majority are solitary or free-living (Roberts et al., 2009). Most species of scleractinian CWCs are found in ocean temperatures that range from 1 to 20°C (Stanley and Cairns, 1988) at shallow to lower bathyal depths, with occasional records as deep as 6328 m (Keller, 1976).

Cold-water corals are particularly useful for unravelling changes in ocean biogeochemistry and circulation in the past (Robinson et al., 2014). They are found in abundance in the Southern Ocean, where other proxy archives such as foraminifera are sparse, and they can be preserved on the seafloor or within sediments for thousands of years (e.g. Burke et al. 2010; Margolin et al. 2014; Thiagarajan et al. 2013). Their depth range often covers intermediate and deep water masses, complementing and extending records from abyssal sediment cores. A record of seawater chemistry throughout their lifetime can be preserved in their carbonate skeleton (Robinson et al., 2014), and their high uranium content allows for application of precise uranium-thorium dating methods (Cheng et al., 2000a; Douville et al., 2010; Lomitschka and Mangini, 1999; Montero-Serrano et al., 2013; Shen et al., 2012, 2008).

The physiology of CWCs and their response to environmental stressors is understudied in comparison to their shallow-water counterparts. However, research volume has grown in recent years, in part because of concerns about the impact of human activity on CWC ecosystems (Guinotte et al., 2006). Water temperature is thought to be one of the most important controls on their range at a global scale (Davies and Guinotte, 2011), but responses to thermal stress have been shown to vary by species (e.g. Büscher et al., 2017; Gori et al., 2016). Cold-water corals rely on a food supply of zooplankton, algal material and particulate organic matter (Duineveld et al., 2007). Hydrography plays an important role in controlling supply of this nutrition, as well as in the dispersal of larvae (Dullo et al., 2008; Miller et al., 2010). Although dissolved oxygen is crucial for corals to maintain aerobic function, the limit of tolerance is unknown, with colonies of the coral *Desmophyllum pertusum* (formerly known as *Lophelia pertusa*) being found to survive at dissolved oxygen concentrations well below the limit suggested in laboratory experiments (Dodds et al., 2007). The extent to which carbonate ion concentration controls CWC range is also disputed. Although 95% of branching CWCs are found above the aragonite saturation horizon (ASH; Guinotte et al., 2006), recent expeditions have also recovered scleractinians from undersaturated waters (e.g. Baco et al., 2017; Thresher et al., 2011). Regional fluctuations in seawater chemistry, productivity, and water mass structure at times in the past are therefore all likely to have exerted some control on regional habitat suitability for CWCs.

1.2 The deglacial Southern Ocean

In this study, we characterise and date a collection of subfossil CWCs from the southern Indian Ocean for the first time and explore the environmental controls on their distribution since the Last Glacial Maximum (LGM; ~23-19 ka). At this time, atmospheric CO_2 concentrations were 80-90 ppm lower than preindustrial values (Monnin et al., 2001). Enhanced carbon storage in the deep ocean resulted from a more effective biological pump (e.g. Wang et al., 2017) and reduced ventilation due to sea ice-induced stratification and/or equatorward wind shifts (Ferrari et al., 2014; Kohfeld and Chase, 2017; Stephens and Keeling, 2000). During the subsequent deglaciation, degassing of CO_2 from the deep ocean is thought to have been responsible for the co-variation in atmospheric CO_2 and Antarctic temperature change (Parrenin et al., 2013), characterised by two ‘pulses’ of CO_2 release separated by a cooling and stabilisation of atmospheric CO_2 during the Antarctic Cold Reversal (ACR; 14.5-12.7 ka; Stenni et al., 2011). Radiocarbon records indicate intervals of breakdown in the deep vertical stratification (Burke and Robinson, 2012; Chen et al., 2015; Siani et al., 2013), while changes in pH conditions reflecting outgassing of CO_2 sourced from deep waters have been reconstructed using boron isotopes (Martínez-Botí et al., 2015; Rae et al., 2018).

The Indian sector of the Southern Ocean is an important location in which to study deglacial ocean biogeochemistry. Frontal movements in this region may have led to changes in the ‘leakage’ of warm, salty eddies from the Agulhas retroflection into the Atlantic Ocean, with implications for Atlantic overturning circulation (e.g. Bard and Rickaby, 2009; Beal et al., 2011; Franzese et al., 2006). In addition, a lag between atmospheric cooling over Antarctica during the ACR (Stenni et al., 2001) and sea surface temperature decline in the southern Indian Ocean (Labracherie et al., 1989) has yet to be fully explained. To date, our understanding of these changes and their global significance has been limited by sparse proxy records from this region, motivating efforts to explore CWCs as a palaeoceanographic archive. By taxonomically cataloguing and dating a new regional sample of intermediate-water CWCs, this study provides a first step towards investigating these processes.

2. Materials and methods

2.1 Sampling location and regional hydrography

Subfossil corals were collected from four seamounts along the Southwest Indian Ocean Ridge (SWIOR), which were surveyed in 2011 during expedition JC066 of the *RV James Cook*. From south to north these were: Coral Seamount (41°21’23” S, 42°50’31” E); Melville Bank (38°31’56” S, 46°45’74” E); Middle of What Seamount (henceforth ‘MoW Seamount’; 37°56’76” S, 50°22’16” E); and Atlantis Bank (32°42’01” S, 57°17’26” E; Fig. 1A; Table 1).

The modern Southwest Indian Ocean (SWIO) is dominated by two major hydrographic features, the Antarctic Circumpolar Current (ACC) and the Agulhas Current system. The Subantarctic Front (SAF), the northernmost front of the ACC, is strongly steered by bathymetry in the SWIO (e.g. Pollard et al., 2007), resulting in a latitude range of 48-43°S (Sokolov and Rintoul, 2009a; Fig. 1A). Further north, a 4°C increase in temperature and a sharp increase in salinity (Fig. 1B) marks the position of the Subtropical Front (STF), the boundary between subantarctic and subtropical surface waters, at around 40°S (Read and Pollard, 2017). The eastward flowing Agulhas Return Current (ARC), which results from overshoot and retroflection of the Agulhas Current south of the African continent, is found in close proximity to the STF in the SWIO (Belkin and Gordon, 1996; Lutjeharms and Van

Ballegooyen, 1988; Read and Pollard, 2017; Fig. 1B). Peak chlorophyll concentrations are found at the ARC/STF, but the highest surface particulate organic carbon concentrations and microorganism abundances are found between the two fronts, in the Subantarctic zone (SAZ; Djurhuus et al., 2017b).

Density surfaces rise upwards to the south, in geostrophic balance with the eastward flow of the ACC, affecting the depth at which specific water masses are present across the SWIO transect (Fig. 1B, C). The subsurface salinity minimum of Antarctic Intermediate Water (AAIW) is found between 500m (Coral) and 1500m (Atlantis) in the southern Indian Ocean and was sampled at all seamounts (Fig. 1B, C). Upper Circumpolar Deep Water (UCDW), a high-nutrient water mass consisting of a combination of Indian and Pacific deep waters, with its upper bound defined by the 27.5 kg m^{-3} neutral density surface (Plancherel, 2012), intersected with sampling at Coral (~900 m) and MoW (~1050 m) seamounts. Lower Circumpolar Deep Water is found in the SWIO at depths of 2 to 3 km (van Aken et al., 2004; Fig. 1C), but such depths were not sampled during this study.

Sampling was opportunistic and not all fossil CWCs seen were collected. All but three of the specimens described here were collected during dives of the *Kiel 6000* Remotely Operated Vehicle (ROV), using manipulator arms, a suction sampler, nets and mini-box corers (Rogers and Taylor, 2011). The remaining specimens were extracted from a megacore sample (JC066_1116), a boxcore sample (JC066_115), and picked up on a dive of the HYBIS towed camera system (JC066_4309). On each seamount, ROV dives were made along deep to shallow transects to analyse the depth and spatial variation of benthic communities. Five ROV dives took place at Coral Seamount, four at Melville Bank, two at MoW Seamount, and three at Atlantis Bank. The 149 scleractinian samples in the collection, of which 122 were solitary, cover a depth range of 172 to 1395 m.

Figure 1: Modern day hydrography proximal to sample locations on the Southwest Indian Ocean Ridge (SWIOR). A, bathymetric map of the sampling region in the Southwest Indian Ocean with positions of fronts marked from north to south: Subtropical Front (STF), Subantarctic Front (SAF), Polar Front, (PF), Southern Antarctic Circumpolar Current Front (green), from Sokolov and Rintoul, (2009). Sample locations are shown with black dots, and the red box highlights the transect along which sections are plotted. B, vertical sections with sampling locations shown with black dots. CTD data accessed from the World Ocean Database, plotted with Ocean Data View (Schlitzer, 2017). From top to bottom are plotted oxygen, labelled with seamount names; temperature, labelled with water masses Subantarctic Mode Water (SAMW), Antarctic Intermediate Water (AAIW) and Upper Circumpolar Deep Water (UCDW); and salinity, labelled with the three regional fronts. The path of the Agulhas Return Current (ARC) combines with the STF as it crosses the SWIOR. Contours of neutral density surfaces (kg m^{-3}) corresponding to water mass boundaries are shown on all three sections. C, schematic section of present-day circulation and positions of frontal jets of the Antarctic Circumpolar Current in the Indian sector of the Southern Ocean. Water masses depicted in addition to SAMW, AAIW and UCDW are subtropical surface waters (STSW); Lower Circumpolar Deep Water (LCDW) and Antarctic Bottom Water (AABW).

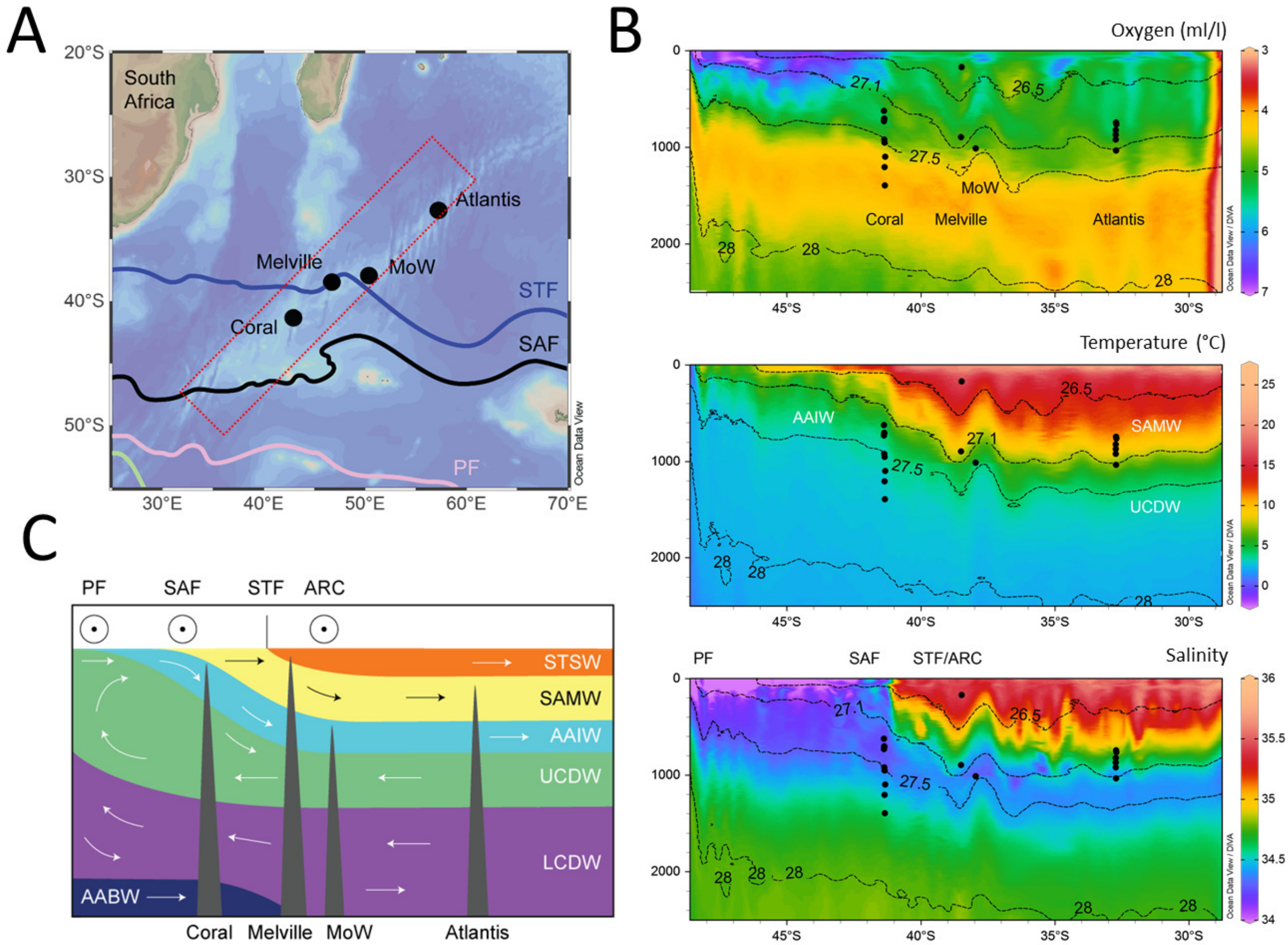

2.2 Taxonomy

Taxonomic identifications of the scleractinian coral specimens were based on monographs which represent the most recent, extensive, and available documents on azooxanthellate Scleractinia. These include Cairns (1982; Antarctic and Subantarctic), Cairns and Keller (1993; SWIO), Cairns (1995; New Zealand), Cairns and Zibrowius (1997; Indonesia), Cairns (2000; Caribbean), Kitahara et al. (2010) and Cairns and Polonio (2013; Indonesia).

Discrepancies in the boundaries and number of biogeographical realms exist between studies of azooxanthellate Scleractinia (see Cairns, 2007) and more recent classifications using benthic marine species and oceanographic proxies (most recently Watling et al., 2013). For the purposes of this study, we use a combination of the two. Atlantis Bank, Melville Bank and MoW Seamount fall within the Indian Lower Bathyal Province proposed by Watling et al. (2013) and the South-West Indian Ocean (SWIO) region following the terminology of Cairns (Cairns, 2007). The STF is designated as the northern boundary for the Subantarctic realm in Cairns (Cairns, 2007), whereas Watling et al. (2013) use the Polar Front. Therefore, Coral Seamount is located in the Subantarctic according to Cairns (Cairns, 2007), but in the Indian Province following Watling et al. (2013). To acknowledge this difference, along with the likelihood that the boundary is transitional, we place Coral Seamount in the 'Subantarctic Transition Zone'.

During taxonomic analysis, specimens were evaluated for preservation of aragonite (1 – highly degraded to 5 – intact) and the relative accumulation of authigenic coating (0 – no coating to 3 – fully coated). These qualitative metrics were combined into a 'preservation factor', by subtracting coating from aragonite preservation (see Appendix 4).

2.3 Laser ablation U-series dating

A total of 122 solitary scleractinian samples were prepared for laser ablation uranium-series age screening in the Bristol Isotope Group (BIG) facilities, following the method developed by Chen et al. (2015) and Spooner et al. (2016). Twenty-one specimens, predominantly of the genus *Balanophyllia,* were too delicate, small, or poorly preserved to proceed with laser ablation dating. Coral samples of a minimum size of 2 x 1.5 mm were cut using a Dremel® tool with a diamond blade, polished flat on one side using four increasingly fine grades of sandpaper, and rinsed with deionised water (18.2 MΩ. cm). Visibly altered or discoloured sections of aragonite were avoided. The samples were then mounted in batches of ~50 into trough-shaped sample holders.

Auto-focussed and pre-programmed 1.1 mm line scans were ablated automatically using 'Chromium 2.1' software linked to the Photon Machines Analyte G2 193 nm laser, which was coupled to a Thermo Finnigan Neptune MC-ICP-MS. The low abundance isotope ^{230}Th was measured in sequence on a central ion counter, with ^{238}U measured simultaneously using Faraday cups (Spooner et al., 2016). Tuning was carried out using NIST 610 glass in order to maximise ^{230}Th signal intensity. An aragonite vein standard from the Salt Wash Graben, Green River, Utah (VS001/1-A) was used to bracket every three samples. Measurements consisted of 50 cycles for samples and bracketing standards, and background intensities were measured for 25 cycles following each standard measurement. Anomalous signal spikes in ^{230}Th were removed before calculation of mean isotope intensities, subtraction of the background intensity, and calculation of the isotope ratios; however, such spikes were rarely observed. Corrections for instrumental, elemental, and isotopic fractionation were applied using bracketing standards. Ratios were used to determine sample age by iteratively solving the age equation using the Newton-Raphson method (Kaufman and Broecker, 1965). Closed system behaviour was assumed, and the known modern seawater $\delta^{234}U_i$ value of 147 ± 7 ‰ (Reimer et al., 2009) was used in the calculation. Previous data indicates age corrections for initial ^{230}Th based on ^{232}Th fall within the usual age uncertainties for this method (Robinson et al., 2014; Spooner et al., 2016), and therefore no correction was made for detrital or seawater Th contribution. Standard errors on the measured ratios, the background measurements, and the errors on the isotope dilution MC-ICPMS isotope ratios of the standards were combined and propagated through each stage of standard corrections (Spooner et al., 2016). Final propagation of errors through the age equation was carried out using a Monte Carlo technique, whereby random Gaussian distributions for each ratio are generated and used to calculate a distribution of possible ages from which the final sample ages and errors are determined. For deglacial age corals these errors range between 500 and 1500 years. The background level was typically 1 count per second, with deglacial corals recording 10-20 cps.

2.4 Isotope dilution U-series dating

Fifty-two subsamples including two full procedural duplicates for combined U, Th, Nd chemistry (~ 0.6 to 5 g) were taken for precise isotope dilution U-series analysis. Physical and chemical cleaning procedures followed the development and assessment of methods performed before in the MAGIC group at Imperial College on cold-water corals (Crocket et al., 2014; van de Flierdt et al., 2010), building on methods developed by Cheng et al. (2000), Lomitschka and Mangini (1999) and Shen and Boyle (1988). All samples were rigorously physically cleaned with a Dremel tool, before undergoing a two-day oxidative-reductive chemical cleaning process. In the BIG laboratory facilities at the University of Bristol, cleaned coral fragments (~0.04 to 1.9g) were then dissolved and spiked with a ^{236}U-^{229}Th mixed spike calibrated to a 4.1‰ (2σ) uncertainty, described further by Burke and Robinson (2012). An iron co-precipitation procedure was utilised to separate trace metals from the carbonate matrix, before U and Th fractions were separated and purified using anion exchange chromatography using columns filled with an Eichrom pre-filter resin and 2 mL Biorad analytical grade anion exchange resin 1-X8 (100-200 mesh).

Uranium and Th isotopes were measured on a Neptune MC-ICP-MS in the BIG laboratories. Bracketing standards were used: for U, an international standard U112a, and for Th an in-house standard 'SGS'. A 45ppb U112a standard solution was used to tune the Neptune prior to U measurement, such that sensitivity for ^{238}U was ~ 250 V/ppm with a variation of < 2%, and between 5 and 95% peak height measured 0.1 amu or less. To correct for mass bias, U112a and SGS were used to bracket U and Th samples respectively. Using these bracketing standards, the activity ratios ^{238}U/^{234}U, ^{232}Th/^{230}Th, ^{232}Th/^{229}Th, and ^{230}Th/^{229}Th were corrected for each sample. The isotopes ^{238}U, ^{236}U and ^{235}U were analysed in Faraday collectors, and ^{234}U on an ion-counter, in measurements of 100 cycles. The low concentration ^{229}Th and ^{230}Th isotopes were analysed on the secondary electron multiplier (SEM) by peak jumping in measurements of 50 cycles. ^{236}U, added as a spike to the Th cut, was measured concurrently on a faraday cup. The latter was used to normalise the ^{230}Th/^{229}Th ratio for signal instability, by measuring ^{230}Th/^{236}U and ^{229}Th/^{236}U (Burke and Robinson, 2012; Chen et al., 2015). The wash solution (i.e. blank) was analysed before every sample run in 10 cycles and subtracted from all absolute values before calculating isotope ratios. Machine accuracy was monitored by measuring Hu84.5 (U) and ThB (Th) standards before each session and every 3-4 samples. An HU84.5 standard was processed with each batch of column chemistry and yielded a long-term external reproducibility for [^{230}Th/^{238}U] of 0.997 ± 0.002, and for [^{234}Th/^{238}U] of 1.0007 ± 0.0008, within error of secular equilibrium (n=50). Errors including machine uncertainties and procedural blanks were propagated into the isotope ratios of ^{234}U/^{238}U, ^{236}U/^{238}U and ^{229}Th/^{230}Th. A Monte Carlo technique was used to propagate the errors of isotope ratios into the final reported uncertainties.

The isotope ^{232}Th was measured in addition to ^{230}Th in order to correct for non-radiogenic sources. Assuming any initial Th incorporated on calcification had a ^{230}Th/^{232}Th ratio equivalent to local modern-day seawater, the measured ^{232}Th can be used to estimate initial ^{230}Th. An initial atomic ^{232}Th/^{230}Th ratio of 12,500 ± 12,500 (2σ) was assumed, corresponding to modern subtropical Atlantic intermediate waters (Chen et al., 2015). This calculation dominates the final error for ages, with measured ^{232}Th correlating with the sample age error due to the greater uncertainty of initial ^{230}Th activity. Measured ^{232}Th ranged from 50 to 3806 ppt, and was the main factor determining the age errors, which ranged from 68 to 985 years for deglacial age corals.

The value $\delta^{234}U_i$ is the deviation (‰) from secular equilibrium of the ^{234}U/^{238}U activity ratio and is used to test for closed-system behaviour of the corals. The $\delta^{234}U_i$ of the SWIO corals ranged from 145.2 to 157.5 ‰. Two of the 50 corals analysed exhibited open-system behaviour with $\delta^{234}U_i$ outside of the modern-day ocean (147 ± 7 ‰; Reimer et al., 2009). Ages of the full procedural duplicates were within error.

3. Results

3.1 Taxonomy

Material from colonial species accounts for 27 of the 149 scleractinian samples, including *Solenosmilia variabilis*, *Madrepora oculata*, *Goniocorella dumosa*, and *Enallopsammia rostrata*. *Solenosmilia variabilis* appears to be the most common species represented among the colonial specimens. However, it is difficult to evaluate the relative abundance of these species as the number of samples cannot be considered representative of the communities found at each seamount.

Of the 122 solitary specimens, the majority represent the family Caryophylliidae, which includes *Desmophyllum dianthus* (*n* = 36), and *Caryophyllia diomedeae* (*n* = 32). Dendrophylliids are also common, including *Balanophyllia gigas*, *Balanophyllia malouinensis*, and *Leptopsammia stokesiana* (*n* = 31). The remaining solitary specimens comprise 13 flabellids (*Flabellum flexuosum* and *Javania antarctica*), two attached *Trochocyathus gordoni*, and free-living specimens of *Deltocyathus sp.* and *Dasmosmilia lymani*. Five solitary and four colonial samples were not identified to genus level due to poor preservation.

An annotated list detailing the 15 scleractinian taxa represented within the new collection is presented below (with further metadata in Appendix 1).

3.1.1 Species List

Order SCLERACTINIA

Family **OCULINIDAE** Gray, 1847

1. *Madrepora oculata* Linnaeus, 1758. Four fragments of this colonial coral, characterised by sympodial budding and anastomosed branches, were collected from patches of coral rubble at Melville Bank and MoW Seamount.

Family **CARYOPHYLLIIDAE** Dana, 1846

2. *Caryophyllia diomedeae* Marenzeller, 1904. Thirty specimens found at Coral Seamount, MoW Seamount and Atlantis Bank shared a hexameral $S1=S2>S3\geq S4$ septal pattern, low, evenly spaced costae, sinuous pali on S3, and a columella formed of fascicular elements (Cairns, 1995; Cairns and Zibrowius, 1997; Kitahara et al., 2010). Two specimens displayed an irregular septal pattern, with 43 and 44 septa in total; similar variations have been described previously from the Atlantic (Zibrowius, 1980) and New Zealand (Cairns, 1995). At least eight specimens had fewer than three columella elements. A few specimens from Atlantis Bank and one from MoW Seamount have highly exert S1-2, up to 5mm (Fig. 2A); however, in most specimens from Coral Seamount and Melville Bank S1-2 were only moderately exert (Fig. 2B). This character arguably places the latter group closer to the range of *Caryophyllia laevigata*, a species described by Kitahara et al. (2010). In this case, the differences amongst specimens was not consistent enough to identify them as separate species, rather than considering a wide range of morphological variation of *C. diomedeae*. Another diagnostic feature, colour banding, was variably expressed and did not necessarily correlate with septal exertness. Finally, it is worth mentioning that most of the Atlantis Bank specimens exhibit fused costal granules near the calicular margin.

3. *Caryophyllia profunda* Moseley, 1881. One specimen of this taxa was collected, from Melville Bank (Appendix 5). Unlike specimens described by Cairns (1995, 1982), all septal edges are straight.

4. *Trochocyathus (T.)* cf. *gordoni* Cairns, 1995. One specimen composed of two budded coralla found at Coral Seamount was assigned to *T.* cf. *gordoni*, although poor preservation, especially of the pali, hampers conclusive identification (Appendix 5). As in the New Zealand specimens (Cairns, 1995), deep intercostal striae are present near calicular

edge, becoming less defined towards the pedicel. Both specimens have an irregular septal arrangement approaching decameral.

5. *Solenosmilia variabilis* Duncan, 1873. Fragments of *S. variabilis* were collected from Coral Seamount and Melville Bank.

6. *Goniocorella dumosa* (Alcock, 1902). Fragments were found at Coral Seamount only. Specimens display straight, cylindrical branches and right-angled budding as described in Cairns (1982).

7. *Dasmosmilia lymani* (Pourtalès, 1871). One specimen was found at Coral Seamount, having fewer columella components than described in Cairns (1995), but a similar septal arrangement, budding pattern, and serrate calicular edge.

8. *Desmophyllum dianthus* (Esper, 1794). The most common species with a total of 36 specimens collected from Coral Seamount, Melville Bank, and Atlantis Bank. They exhibit a wide range of variation within the species, from small juvenile to large adult specimens, straight to slightly bent corallum, and low to highly exert septa. A few specimens from Atlantis Bank are distinct in that they most clearly bear the characteristic features of *D. dianthus*: clear, ridged costae; highly exert, flared septa and finely granular theca (Fig. 2C; Cairns, 1982).

Family **DELTOCYATHIDAE** Kitahara et al., 2012

9. *Deltocyathus* sp. Milne Edwards and Haime, 1848. A single, small, free living specimen was found at Melville Bank. The specimen exhibits diagnostic characters of the genus *Deltocyathus*, having pali before septa of all but first cycle and axial edges of higher septa (S4) joining to faces of adjacent septa (S3). However, the poor preservation of the specimen hampers its identification to species level.

Family **FLABELLIDAE** Bourne, 1905

10. *Flabellum flexuosum* Cairns, 1982. Three specimens were collected at Coral Seamount. They exhibit a thin, porcellaneous theca, and sinuous, wrinkled edges of the inner septa (Cairns, 1982, Appendix 5). However, none have a fifth septal cycle.

11. *Javania antarctica* (Gravier, 1914). Seven specimens from Coral Seamount and one from Melville Bank were collected. Although similar in morphology to *F. flexuosum*, these specimens were distinguished by their distinctive chevron growth lines peaking at intersections with 'costae', as described in Cairns (1982; Appendix 5). Only one specimen displayed a rudimentary fifth septal cycle.

Family **DENDROPHYLLIIDAE** Gray, 1847

12. *Balanophyllia gigas* Moseley, 1881. Twenty-one specimens representing this species were found at Coral Seamount. It is likely that all specimens are juvenile, as none express a full Pourtalès plan septal arrangement and they are much smaller than specimens described from New Zealand (Cairns, 1995). The presence of banded epitheca above the synapticulotheca (Cairns and Zibrowius, 1997) is variable. They all have in common a deep, narrow fossa and relatively narrow septa (Appendix 5).

13. *Balanophyllia malouinensis* Squires, 1961. A total of five specimens were recovered from Coral Seamount and Melville Bank. They were distinguished from *B. gigas* by having a thick, spinose synapticulotheca and a shallower fossa with a larger columella (Cairns, 1982; Appendix 5). Like the *B. gigas* specimens, the septa are arranged only in a rudimentary Pourtalès plan.

14. *Leptopsammia stokesiana* Milne Edwards and Haime, 1848. Five specimens were found at Coral Seamount. Although similar in size and morphology to the other solitary dendrophylliids in the collection, these do not have a Pourtalès plan septal arrangement (Cairns and Zibrowius, 1997).

15. *Enallopsammia rostrata* (Pourtalès, 1878). In total four fragments of this robust, uniplanar colonial coral were found at Melville Bank and Atlantis Bank.

Figure 2: Morphological variability of CWCs across seamount transect. Calice and corallum of *Caryophyllia diomedeae* from A, Atlantis Bank (JC066_3741) and B, Coral Seamount (JC066_122); and calice and corallum of *Desmophyllum dianthus* from C, Atlantis Bank (JC066_3718) and D, Coral Seamount (JC066_127).

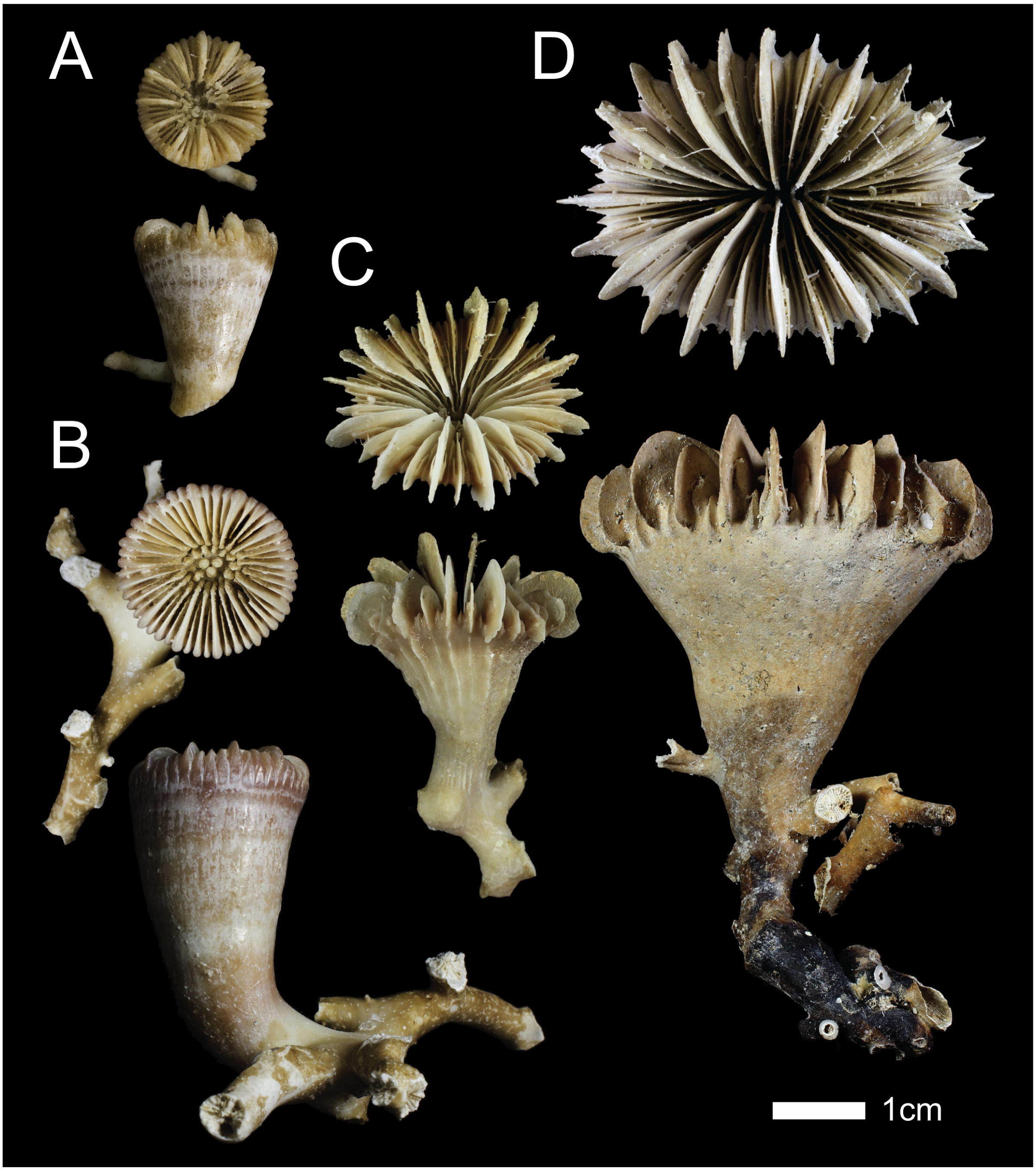

3.1.2 Taxonomic distribution

All solitary CWCs except the *C. profunda*, which was collected at the summit of Melville Bank at 172 m water depth, were found between 600 and 1400 m (Figs. 1, 3), covering modern SAMW, AAIW, and UCDW depths, although the latter was only represented by specimens from Coral Seamount. This depth range is in part constrained by the position of the seamount summits, particularly at MoW Seamount (1100 m) and Atlantis Bank (750 m), and the maximum depth of the ROV surveys (see Table 1 and Fig. 3).

Table 1: Location, bathymetry, and number of specimens from SWIO seamounts

Seamount	Latitude (°S)	Longitude (°E)	Summit (m)	Max survey depth (m)	Solitary CWC specimens	CWC specimens dated
Coral	41°21'23" S	42°50'31" E	175	1395	89	72
Melville	38°31'56" S	46°45'74" E	91	1276	9	5
MoW	37°56'76" S	50°22'16" E	876	1414	7	7
Atlantis	32°42'01" S	57°17'26" E	690	1117	17	17

At Coral Seamount, the greatest number (n = 89) and diversity of CWCs was found, with 9 out of 11 solitary species represented (Fig. 3). Samples were collected between 624 and 1395 m, intersecting the boundary between AAIW and UCDW at ~900 m. Most corals of this collection were recovered at ~700 m, where 27 of the 30 Dendrophylliidae specimens are found, and ~1200 m, dominated by Caryophylliidae.

At Melville Bank and MoW Seamount, solitary CWC specimens were found near to the modern-day SAMW/AAIW and AAIW/UCDW boundaries, respectively (Fig.1B). Nine specimens from Melville Bank represent a minimum of five species (Fig. 3). All seven CWCs from MoW Seamount are *C. diomedeae*. At both seamounts the ROV transect extended a few hundred metres below where the deepest CWCs were found.

The 17 CWC specimens from Atlantis Bank span the full depth range surveyed from 700 to 1100 m. *Desmophyllum dianthus* and *C. diomedeae* were the only solitary species collected in this locality (Fig. 3).

A range of preservation of the skeletal aragonite was observed, from near-perfect to heavily bored and/or dissolved. Corals were often found coated with grey-brown authigenic deposits. No significant correlation was found between water depth and individual coral mass or preservation factor (Fig. 4A). On the whole, coating levels and aragonite degradation appear to be positively correlated, i.e. poor aragonite preservation was linked to high coating levels (see Appendix 4).

Figure 3: Depth distribution of subfossil CWCs at each seamount, colour coded by species. Seamount summits and the deepest vertical extent of ROV surveying are represented by dashed grey lines. Modern day water mass boundaries between Subantarctic Mode Water (SAMW), Antarctic Intermediate Water (AAIW) and Upper Circumpolar Deep Water (UCDW) are defined using the depths of neutral density for AAIW (27.1< γ_n < 27.5; Plancherel, 2012) at each seamount, from World Ocean Database CTD data.

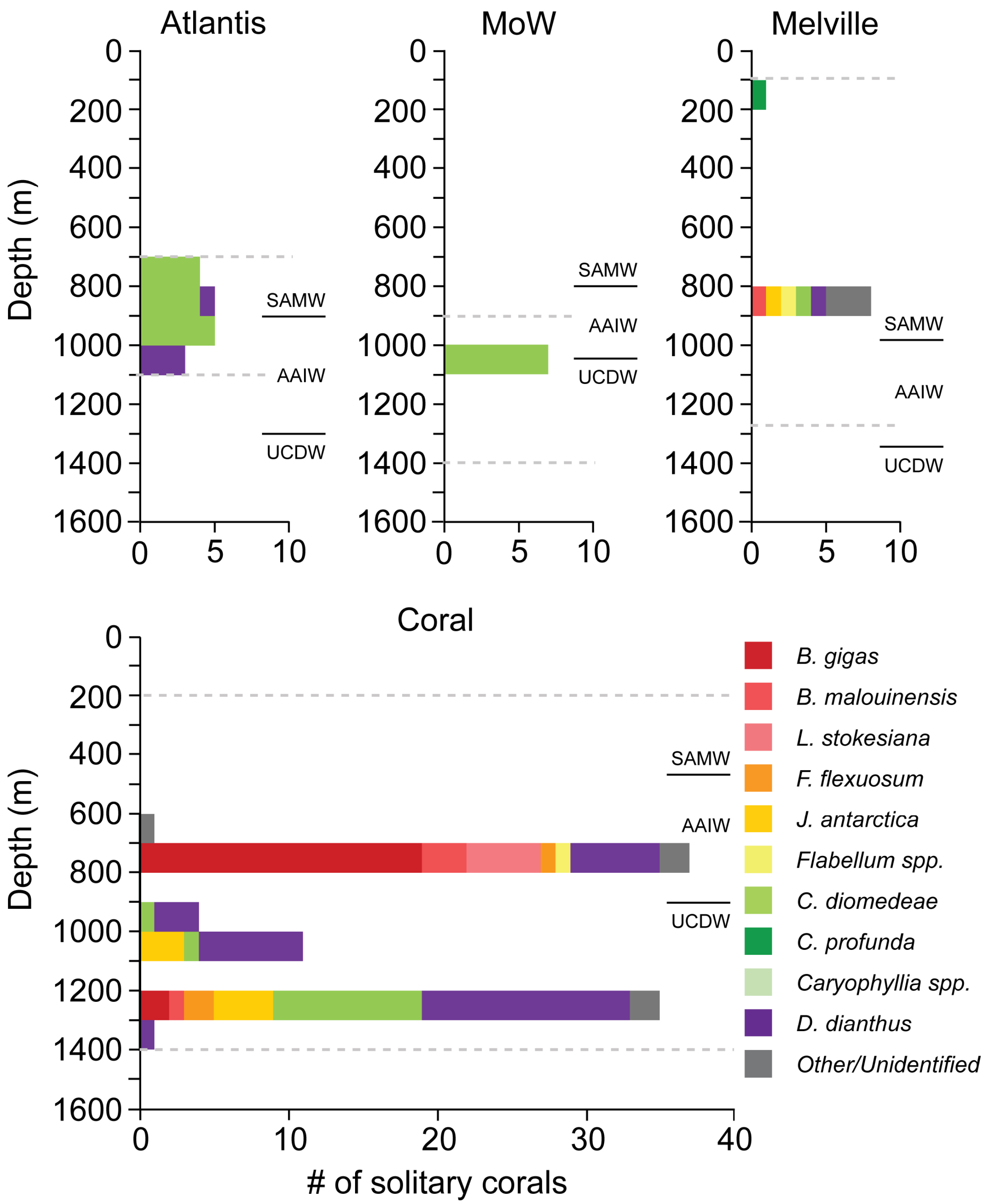

3.2 Ages

The 101 dated CWCs range in age from the LGM to the modern day (Fig. 6), except for a single 140 ka specimen from Melville Bank. Isotope dilution U-series dating of 50 of the samples demonstrated the accuracy of the laser ablation technique, with a close correlation and 33 samples giving ages within error of the laser ablation dates (Fig. 5). Only late Holocene CWCs were found at Atlantis Bank, whereas both Holocene and deglacial specimens were found at Coral Seamount, Melville Bank and MoW Seamount. There are relatively few samples from the mid-Holocene (~5 ka) and the Last Glacial Maximum (19 – 25 ka). The most well preserved and largest CWCs date from periods of greatest abundance, whilst the few corals found during the LGM and early- to mid-Holocene are poorly preserved (Fig. 4B).

Figure 4: Relationship of caryophylliid mass and preservation factor to A, depth and B, age, at all seamounts for the two most prevalent species (colour coded). Preservation factor is a qualitative metric that takes into account the amount of ferromanganese coating and aragonite dissolution, and ranges from -2 (least well preserved) to 5 (intact).

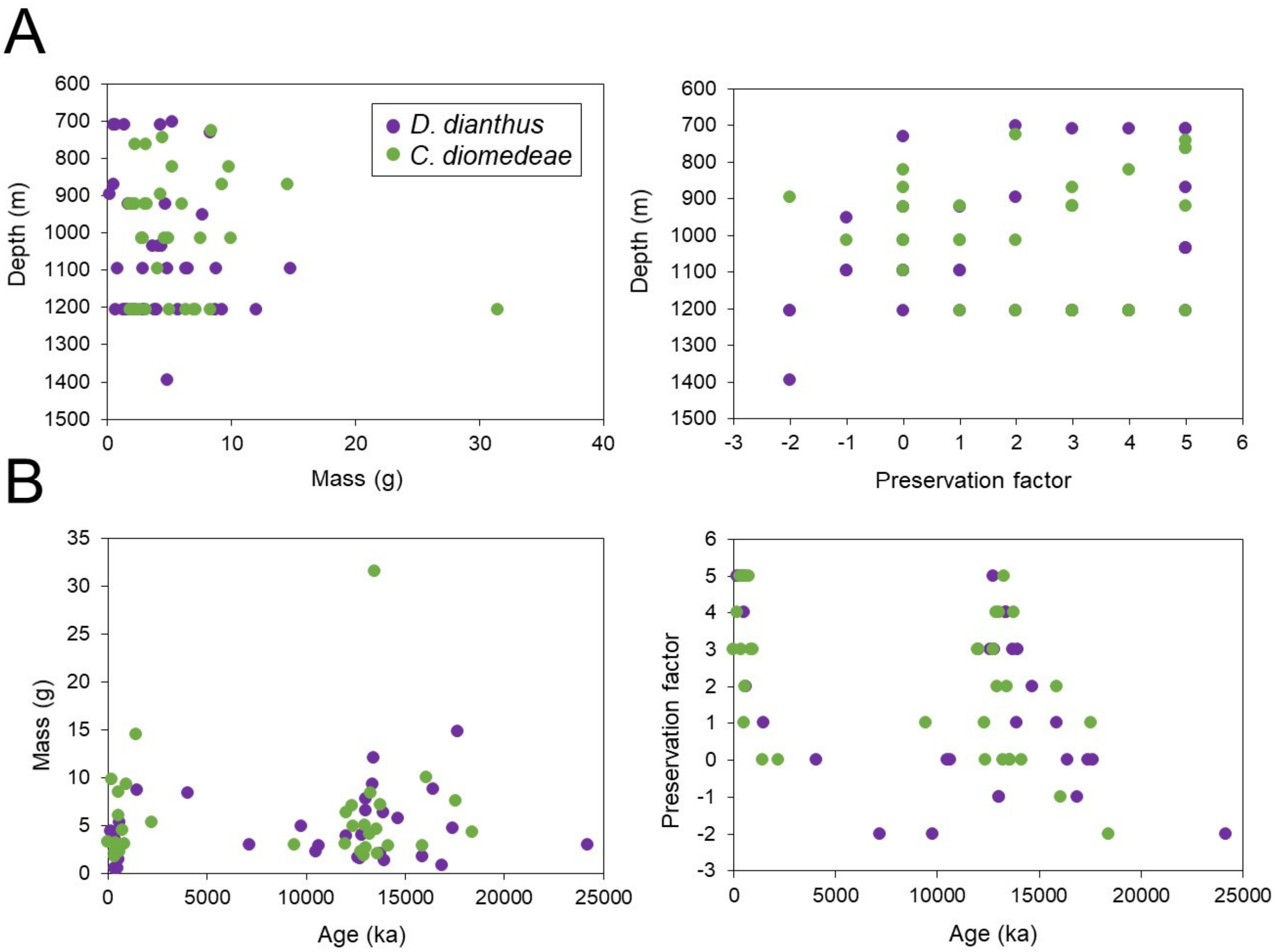

Figure 5: Comparison of laser ablation (LA) and isotope dilution (ID) U-series ages for 50 cold-water corals from south-west Indian Ocean seamounts. The 1:1 line (solid) and trendline (dashed) are shown.

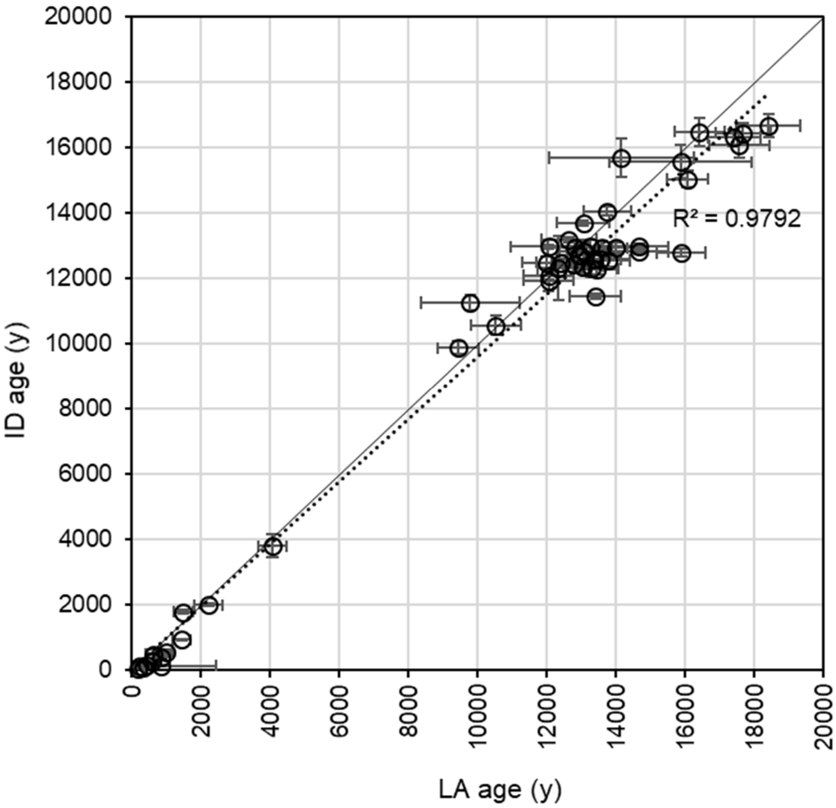

4. Discussion

4.1 Taxonomy

4.1.1 Range extensions

Previous surveys of CWC diversity in the region include the works of Cairns and Keller (1993) for southern Africa and Madagascar, and Cairns (1982) for the Antarctic and Subantarctic. In the former, the scleractinian fauna is described as having influence from Pacific, and to a lesser extent, Atlantic faunas, in addition to species endemic to the Indian Ocean. The distribution of the species in this collection and their proposed extensions are shown in Table 2. Of the 15 scleractinian deep-water coral species found in this study, six have already been recorded from the SWIO and/or Subantarctic regions: the cosmopolitan species *C. profunda, D. dianthus*, *M. oculata, E. rostrata* and *S. variabilis,* in addition to *G. dumosa*, which is Indo-West Pacific (Cairns and Keller, 1993; Cairns, 1982). The genus

Deltocyathus is also widely distributed in all oceans; although as we were not able to identify the specimen to species level, future explorations and collection of well-preserved specimens from these localities will be needed to allow a better knowledge of this genus in the region. The remaining eight species represent extensions to their previously documented ranges (Table 2), increasing the known scleractinian diversity of the SWIO and Subantarctic Transition Zone. Surprisingly, none of the Dendrophylliidae or Flabellidae species described previously from the SWIO (Cairns and Keller, 1993) were observed in this collection.

The connectivity of Indian and Pacific surface waters through the Indonesian throughflow led Cairns and Keller (1993) to predict that representation of the ‘Indo-West Pacific’ fauna would increase with further exploration in the SWIO. The first record of three species in the Indian Ocean supports that prediction: *T. gordoni* (known only from the Kermadec Islands, New Zealand / Kerguelen province; Cairns, 1995), *B. gigas* (West Pacific and New Zealand / Kerguelen; Cairns and Zibrowius, 1997), and *D. lymani* (warm temperate Pacific and Atlantic; Cairns, 2000). Connectivity of the Southern Ocean through the ACC could also have contributed to the spread of these species. All three species were found at depths (700-1200 m) which extend their bathymetric distribution to deeper waters (Table 2).

The seamounts cover a transitional biogeographic zone between the Indian and Subantarctic regions, which is reflected both by the extension of species from the south into the Indian province, and from temperate regions into the Subantarctic. Known previously only from the Antarctic continent (Cairns, 1982), *F. flexuosum* was found north of the SAF at Coral Seamount. There is evidence that genetic dispersal of CWCs follows ocean density gradients and is less likely to occur vertically (Dullo et al., 2008; Miller et al., 2011). It is possible that *F. flexuosum* extend their distribution up to the SWIO thanks to northwards transport via intermediate waters, as it is found below its previously known depth range between 700 and 1200 m. *Javania antarctica* and *Balanophyllia malouinensis*, whose ranges were recently extended from the Antarctic / Subantarctic (Cairns, 1982) to the southwest Atlantic (Cairns and Polonio, 2013), were also found at Coral Seamount as well as Melville Bank. Water temperature at Atlantis Bank may be above the tolerance of these Antarctic species. It is also possible that the ARC acts as a dispersal barrier to the Indian Ocean for CWC larvae, in a similar manner to the ACC (e.g. Dueñas et al., 2016); although to our knowledge this has not yet been modelled or evaluated.

Neither *C. diomedeae* nor *L. stokesiana* were listed in Cairns and Keller's (1993) SWIO monograph, but both have been found previously in the Indian and West Pacific provinces (Cairns and Zibrowius, 1997; Kitahara et al., 2010). As they were collected from Coral Seamount, their ranges are extended into the Subantarctic Transition Zone. This find also extends the range of *L. stokesiana* from shallow to bathyal waters.

Table 2: Distribution of subtropical and Subantarctic Transition Zone (TZ) south-west Indian Ocean (SWIO) and Indian Ocean (IO) Bathyal Province azooxanthellate Scleractinia discussed in this study. Depth range in bold signifies a proposed bathymetric extension. MoW: Middle of What seamount.

			TZ	SWIO										New record		
Species	Antarctic	Subantarctic	Coral Seamount	Melville Bank	MoW seamount	Atlantis Bank	Other SWIO sites	Indian	West Pacific	New Zealand / Kerguelen	Atlantic	Cosmopolitan	Depth (m) (worldwide)	SWIO *sensu* Cairns (1982)	IO Bathyal Province *sensu* Watling et al. (2013)	Subantarctic Transition Zone
Madrepora oculata		x		x	x		x	x	x	x	x	x	55-1950			
Caryophyllia diomedeae			x		x	x		x	x	x	x		225-2200	x		x
Caryophyllia profunda	x	x		x			x	x		x		x	35-1116			
Trochocyathus (T). gordoni			x							x			**398-732**	x	x	x
Solenosmilia variabilis	x	x	x	x			x	x	x		x	x	220-2165			
Goniocorella dumosa		x	x				x	x	x	x			88-1488			
Dasmosmylia lymani			x						x	x	x		**37-1207**	x	x	x
Desmophyllum dianthus	x	x	x	x		x	x	x	x	x	x	x	8-2460			
Deltocyathus sp.				x			x	x	x				44-5080			
Flabellum flexuosum	x		x										**101-1207**	x	x	x
Javania antarctica	x		x	x							x		53-1280	x	x	x
Balanophyllia gigas			x						x	x			**90-1200**	x	x	x
Balanophyllia malouinensis	x	x	x	x							x		**75-1207**		x	
Leptopsammia stokesiana			x					x	x				**46-710**	x		x
Enallopsammia rostrata		x		x		x	x	x			x	x	110-2165			

4.1.2 Spatial variability

The seamounts in the SWIO form a transect across contrasting hydrographic and productivity regimes, with peak chlorophyll concentrations nearest to the ARC/STF frontal zone (Melville and MoW seamounts; Read et al., 2000). During the JC066 cruise, surface nutrient and particulate organic carbon (POC) concentrations were found to be highest at Coral Seamount (Djurhuus et al., 2017b), as was microorganism abundance (Djurhuus et al., 2017a). These features, along with the systematic variability in microbial community structure, led Djurhuus et al. (2017a) to separate the region into three biogeographic zones – south (Coral Seamount), convergence zone (Melville Bank and MoW Seamount), and north (Atlantis Bank). At depth, water masses were considered more influential, with similar taxa occurring below 200 m across the seamounts (Djurhuus et al., 2017a). The limited sample size and opportunistic nature of the sampling in this study makes a quantitative assessment of spatial variability patterns in CWCs difficult. Because of the differing seamount heights, the maximum depth of the ROV, and cruise time constraints (i.e. opportunistic sampling of subfossil CWCs), the full depth range of CWCs may not have been surveyed (Table 1). Nevertheless, notable variations in coral diversity are present in the dataset and warrant exploration.

Firstly, a larger number of samples and greater species diversity in subfossil Scleractinia was found at Coral Seamount relative to the other seamounts (Fig. 3). This could be explained by sampling bias, as ROV bottom time was approximately 35 hours at Coral, longer than at Melville (~ 29 hrs), Atlantis (~ 26 hrs) and MoW (~11 hrs); at MoW sampling was severely hampered by turbulent conditions. However, a wide variety of habitats was noted from video footage at Coral Seamount (Rogers and Taylor, 2011), and video surveys suggest it hosts the greatest diversity and number of species for corals and sponges (Frinault, 2017). It was also found to host the largest microbial community (Djurhuus et al., 2017a) and the highest surface chlorophyll concentrations of the four seamounts (Djurhuus et al., 2017b). There are several factors which could contribute to the favourability of Coral Seamount as a habitat for

CWCs. As a result of its position south of the STF, water temperatures at Coral were ~ 3°C to 5°C at the depths of coral collection (~ 600 – 1400 m; Fig. 1B). In contrast, at the three more northerly seamounts, temperatures above 12°C occur down to ~ 600 m and only fall below 5°C at ~ 1100 m. As scleractinian CWCs are most commonly found in waters of 4-12°C (Roberts et al., 2006), Coral Seamount may provide more suitable thermal conditions over a wider depth range. The location of Coral Seamount south of the STF, in the transition between two biogeographic provinces, could also contribute to its high diversity. In contrast, at the subtropical site of Atlantis Bank no flabellids or dendrophylliids were collected. The temperature profile at Atlantis Bank below 200 m is similar to Melville Bank, where dendrophylliids were present, but additional factors such as low POC concentration could reduce the viability of certain species at Atlantis Bank, even those known from temperate locations such as *B. gigas* and *L. stokesiana* (Cairns, 1995; Cairns and Zibrowius, 1997).

We also find some evidence of within-species variations between the four seamounts. A 'robust' morph of *C. diomedeae*, with exert, transversally ridged and laterally protruding septa was dominant at Atlantis Bank (Fig. 2A), whereas most specimens at Coral Seamount had less exert septa (Fig. 2B). It is worth noting that the Atlantis specimens are dated to the late Holocene, whereas all *C. diomedeae* from Coral Seamount are deglacial in age. A few specimens at Melville Bank and MoW Seamount share features of these two end members. To some extent a similar pattern is seen in *D. dianthus;* three specimens at Atlantis Bank have particularly flared septa and well-defined costae (Fig. 2C), whilst specimens to the south display a smoother corallum with less exert septa (Fig. 2D). These discrepancies exist between specimens of the same age at Atlantis Bank and Coral Seamount. Wide intraspecific variability is a characteristic of both of these species (Addamo et al., 2015; Kitahara et al., 2010), and could be due to phenotypic flexibility in different environmental conditions, or genetic isolation and divergence (Miller et al., 2011). Either explanation could apply here, but since the variation could best be described as a spectrum across the seamounts, it seems more likely to be a response to environmental conditions such as temperature and/or food availability.

Overall, the variations in the subfossil CWC collection north and south of the STF give some support to the idea of biogeographic zonation. But there are also similarities in the species found, which may result from the water mass connectivity at depth. Without surveys and phylogenetic analyses on modern CWCs, the importance of these two factors cannot be quantified. The rarity of expeditions to the area and the disturbance of organisms and substrate because of trawling in the SWIO (Rogers and Taylor, 2011) are likely to inhibit these more robust investigations.

4.2 Temporal shifts in CWC populations

Uranium-series dating of the SWIO collection reveals variability in the distribution and diversity of CWCs over the past 25,000 years. Here we discuss patterns of coral abundance in relation to deglacial climate and regional oceanographic changes (Figs. 6-8).

Figure 6: Depths and ages of subfossil CWCs at A, Atlantis Bank; B, Melville Bank (triangles) and Middle of What Seamount (dots) and C, Coral Seamount, coloured coded by taxonomic category. Precise ages are given for samples which underwent isotope dilution U-series dating, and laser ablation ages are used for all other samples (see Appendices 1-3). Grey and white bars indicate the timings of the Holocene, Younger Dryas (YD), Antarctic Cold Reversal (ACR), Heinrich Stadial 1 (HS1), and the Last Glacial Maximum (LGM). The depths of boundaries between Subantarctic Mode Water (SAMW), Antarctic Intermediate Water (AAIW) and Upper Circumpolar Deep Water (UCDW) at each seamount are indicated by black lines.

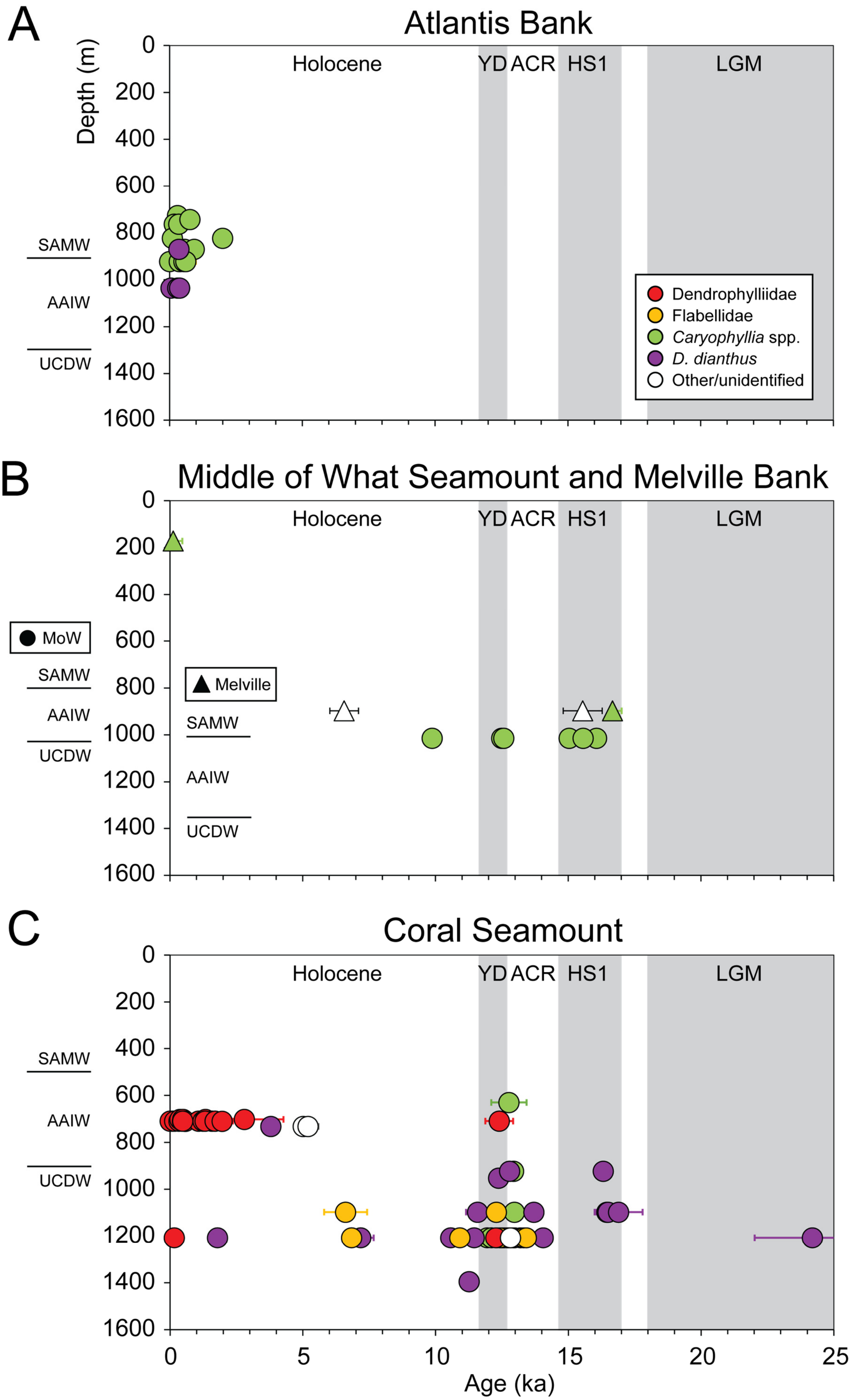
A
Atlantis Bank
Depth (m)
Holocene
YD
ACR
HS1
LGM
SAMW
AAIW
UCDW
Dendrophylliidae
Flabellidae
Caryophyllia spp.
D. dianthus
Other/unidentified
B
Middle of What Seamount and Melville Bank
MoW
Melville
C
Coral Seamount
Age (ka)
0
200
400
600
800
1000
1200
1400
1600
0
5
10
15
20
25

4.2.1 The Last Glacial Maximum

One of the most notable aspects of the SWIO coral record is the absence, bar one *D. dianthus* specimen, of samples dating to the LGM (Figs. 5, 6). Preservation bias cannot be ruled out, though an older specimen, dated from MIS 6 (142 ± 8 ka) was found, and much older *D. dianthus* specimens from the subpolar region have previously been recorded (Burke and Robinson, 2012). It is unlikely that food supply was limiting; opal and organic carbon flux increases point to higher export production in the SAZ of both the Atlantic (Martínez-García et al., 2014) and Indian oceans (Dezileau et al., 2003) during the glacial. In general, coral recruitment will not occur unless there is a consistent supply of larvae to the region in question. Hence, the LGM absence of CWCs could indicate the existence of a barrier to larval dispersal into the SWIO at that time, for example, the ACC. In the Drake Passage, glacial age CWCs were found almost exclusively in the Antarctic Zone, leading Margolin et al. (2014) to suggest that the Polar Front posed a barrier to larval transport further north. As samples south of the Polar Front were not sampled in the SWIO, it is difficult to make direct comparisons. If larval dispersal to the SWIO seamounts from south of the ACC was inhibited during the glacial, a subsequent expansion of CWCs would require either a weakening of the ACC flow, or a northward shift of the Southern Ocean fronts. Reconstructions of glacial flow speeds suggest a similar current speed (Mastumoto et al., 2001; McCave et al., 2014) or lower flow speed (Roberts et al., 2017) compared to the Holocene. In terms of frontal position, it is likely that the Polar Front occupied its most northerly position during the LGM, moving poleward during the early deglacial (Barker et al., 2009; De Deckker et al., 2012). Therefore, evidence for the Polar Front and ACC posing a greater barrier to CWC distribution in the Subantarctic and Subtropical Southern Ocean during the LGM is unconvincing. If the deglacial appearance of CWCs resulted from enhanced larval transport from lower latitudes, we would perhaps expect to see earlier occurrences at Atlantis Bank. The circumpolar transport of the ACC, the influence of the ARC, and the overturning circulation (Henry et al., 2014) could all have provided routes for widespread larval dispersal throughout the glacial and in the modern day.

Given the likelihood of an adequate food supply and open routes for larval dispersal northwards, we suggest that environmental boundary conditions limited CWC growth in the SWIO during the LGM. A broad consensus exists that a large proportion of glacial CO_2 was stored in the deep ocean as a result of a more effective biological pump and reduced deep ocean ventilation (Kohfeld and Chase, 2017). The resulting decrease in carbonate ion concentration and shoaling of the ASH (Sigman et al., 2010; Yu et al., 2010) may therefore have reduced the ability of CWCs to calcify, especially in deep waters. This environment may also have caused dissolution of existing subfossil CWCs, explaining the absence, bar one, of corals dating to earlier periods of more favourable climate conditions. Trace metal evidence also suggests intermediate waters were depleted in dissolved oxygen (Durand et al., 2018; Jaccard et al., 2016), likely resulting from stratification and increased isolation from the atmosphere (Burke et al., 2015). In addition, temperatures in intermediate waters are estimated to have been 3-5°C lower at this time compared to the Holocene, and deep waters ~3°C cooler than the deglacial maxima (Fig. 7E; Elmore et al., 2015; Roberts et al., 2016). We therefore suggest that a shoaled ASH and cool, deoxygenated intermediate waters contributed to unfavourable conditions for CWC growth during the glacial, outcompeting any possible benefits of enhanced food supply. Glacial subfossil coral abundance is also low south of Tasmania (Fig. 7B; Thiagarajan et al., 2013) and in the subantarctic Drake Passage (Fig. 7C; Margolin et al., 2014), supporting a consistent circumpolar response of CWCs to the glacial boundary conditions.

4.2.2 The early deglacial, Heinrich Stadial 1

The early deglacial appearance of CWCs at the three seamounts south of the STF (Coral, Melville and MoW; Fig. 6) is concurrent with the onset of Antarctic warming and Heinrich

Stadial 1 (HS1; 18-14.7 ka; Fig. 7A) ~18 ka ago. During this time interval, release of a deep inorganic carbon pool through processes in the Southern Ocean is thought to have contributed to the atmospheric CO_2 rise (Marcott et al., 2014). Increases in benthic $\delta^{13}C$ (Ninnemann and Charles, 2002; Roberts et al., 2016), reductions in deep water ventilation age (Burke and Robinson, 2012; Skinner et al., 2010), and increases in abyssal carbonate ion concentrations (Yu et al., 2010) all support the deep ocean ventilation hypothesis. These processes may have resulted in a deepening of the ASH and improved conditions for CWC calcification. However, such changes in the deep and abyssal oceans may not have reached depths less than 1400 m at which CWCs were found; on the contrary, depletions in intermediate water radiocarbon have been reported (Bryan et al., 2010; Romahn et al., 2014), likely reflecting transient transport of the deep stored carbon into shallower levels before its release to the atmosphere.

During HS1, increased oxygenation is recorded in the deep Southern Ocean (Jaccard et al., 2016) and the intermediate northern Indian Ocean (Jaccard and Galbraith, 2012), which would have contributed to improving conditions for CWC growth. It is also possible that coral population growth was boosted by increased food supply in the form of sinking particulate organic matter, given the increase in opal flux in the Pacific and Atlantic sectors of the Southern Ocean at this time (Anderson et al., 2009; Fig. 7D). We therefore suggest that the simultaneous appearance of subfossil corals in the SWIO, Tasmania (Thiagarajan et al., 2013), and the subantarctic Drake Passage (Margolin et al., 2014) during HS1 could have been facilitated by increasing oxygen concentrations and food supply, but was still limited by carbonate chemistry at mid-depths, particularly in the Indian and Pacific sectors of the Southern Ocean. Cold-water coral growth also seems to have been enhanced off the coast of Brazil during this time, potentially as a result of increased upwelling and food supply (Mangini et al., 2010).

4.2.3 The late deglacial

The greatest abundance of subfossil CWCs in the SWIO occurs in the late deglacial (33 specimens; Figs. 6, 7A), predominantly within the Younger Dryas (YD), between 13.5 and 11.5 ka. During this period, Coral Seamount supported a diverse community of at least seven solitary scleractinian species including *C. diomedeae*, *F. flexuosum* and *J. antarctica*. Notably, this peak in abundance is located at UCDW depths (~ 900-1400 m at Coral Seamount), with only four specimens found at modern-day AAIW depths. Late deglacial abundance peaks also occur at modern UCDW depths in the Tasmanian (Fig. 7B) and Drake Passage collections (Fig. 7C).

As AAIW depths appear to be preferable for CWCs in the late Holocene, it is tempting to explain their presence deeper in the water column during the deglaciation by a deepening of AAIW and displacement of the lower-oxygen UCDW. Water mass boundaries will have occupied deeper positions in the water column as a result of lower sea level; however this effect can only account for ~60 m displacement between the YD and Holocene, rather than the observed 200 – 500 m depth shift observed at Coral Seamount. Because of the sloping isopycnals in this region (Fig. 1), a more southerly position of the SAF would effectively deepen AAIW at the SWIO and seamounts and around Tasmania. However, reconstructions suggest the SAF occupied a similar position to the present day during the late deglacial (De Deckker et al., 2012; Roberts et al., 2017). A deepening of AAIW would also not explain the relative lack of corals from < 900 m. Hence, we consider other possible controls on the CWC distribution.

Oxygen concentrations below ~145 µmol/kg have been shown to limit respiration of certain *D. pertusum* (=*L. pertusa*) specimens in laboratory experiments (Dodds et al., 2007). An early- to mid-Holocene decline of CWC populations in the Mediterranean has been linked to a fall in oxygenation below ~180 µmol/kg (Fink et al., 2012), and low oxygen also appears to affect the distribution of CWCs in the late Holocene south of Tasmania (Thiagarajan et al., 2013). Elevated oxygen concentrations recorded in the intermediate northern Indian Ocean (Jaccard and Galbraith, 2012) and the deep Southern Ocean (Jaccard et al., 2016) during the period of relative CWC abundance in the SWIO, suggest a plausible role for oxygenation. Intermediate water pH in the Drake Passage also peaked during this time (Rae et al., 2018). Although these ocean chemistry reconstructions cover density intervals below the corals in this collection, chemical changes could feasibly have been communicated to UCDW depths.

Increased food availability is also an important driver of CWC fitness (Naumann et al., 2011), and for cold water corals this consists of particulate organic carbon and microorganisms (Roberts et al., 2009). There is clear evidence for higher export production in the Antarctic Zone of the Atlantic Southern Ocean at 13-11.5 ka, coeval with the CWC abundance peak (Anderson et al., 2009; Fig. 7D). Enhanced export production could have resulted in higher POC concentrations at depth, supplying CWCs with nutrition in the SAZ. However, the most likely path for northward transport of this food supply would be in surface currents and AAIW via Ekman pumping (Marshall and Speer, 2012). In the SWIO, UCDW flows northward above 1500 m (McCave et al., 2005), so could also have advected POC northwards towards Coral Seamount, but it seems unlikely that it would have been the main conduit. Productivity peaks and an associated increase in food availability may explain the overall increase in abundance of CWCs during the late deglacial period, but do not explain the apparent preference for UCDW depths.

Global scale modelling of CWC distribution shows a strong correlation with temperature (Davies and Guinotte, 2011), and although a lower limit has not been tested in laboratory experiments (to our knowledge), CWCs are rarely found below temperatures of 1°C (Stanley and Cairns, 1988). *Desmophyllum dianthus* has been found in waters as cold as 1°C in the Drake Passage (Margolin et al., 2014), and in the late Holocene SWIO we find specimens at depths corresponding to modern temperatures of between ~16°C and 3°C. In the subantarctic

South Atlantic, Mg/Ca-derived temperature reconstructions suggest that intermediate waters were colder than deep waters for much of the deglacial interval, initially at -1 to -2°C and remaining below 1°C until the early Holocene (Roberts et al., 2016; Fig.7E). Deep waters were warmer at around 0-2 °C during the early deglacial and reached a peak of 4°C between 13 and 11ka, with a stable vertical density stratification being conserved because of higher salinities at depth (Adkins et al., 2002; Roberts et al., 2016). Therefore, we propose that low temperatures may have been an important factor in the relative paucity of CWCs from AAIW depths during the deglacial. In addition, we note that deep waters in the Indian, Pacific, and Atlantic oceans reached a peak in carbonate ion concentration between 15 and 10 ka (Yu et al., 2010). Such globally enhanced carbonate ion concentrations would have deepened the ASH, and possibly enabled the expansion of CWCs into CDW, which by that time had reached a warmer and more optimal temperature.

In summary, we propose that increased oxygenation, a deepened ASH, warmer temperatures, and a peak in regional food supply created suitable conditions for CWC growth in UCDW depths during the YD. In contrast, CWCs may have been unable to survive at AAIW depths until the salinity-controlled stratification broke down and temperatures increased in the Holocene.

Figure 7: Number of cold-water corals (CWCs) per 1000-year age bin at three Southern Ocean locations, coded by water mass, with Antarctic Intermediate Water (AAIW) in blue and Upper Circumpolar Deep Water (UCDW) in purple. Precise ages are given for samples which underwent isotope dilution U-series dating, and laser ablation ages are used for all other samples (see Appendices 1-3). A, SW Indian CWCs (this study), overlain with the West Antarctic Ice Sheet (WAIS) Divide Core $\delta^{18}O$ record and 11-point moving average (WAIS Divide Project Members, 2015), and composite CO_2 record with 5-point moving averages from WDC (orange, Marcott et al., 2014) and EPICA (red, Monnin et al., 2001). B, Tasmanian *D. dianthus* abundances (Thiagarajan et al, 2013), assigned to water mass following Hines et al. (2015; AAIW 500-1500m). C, Drake Passage *D. dianthus* abundances, using water mass designations from Margolin et al. (2014). D, Opal flux record from South Atlantic core TN057-13-4PC (53.1728°S, 5.1275°E, 2848m; Anderson et al., 2009). E, Mg/Ca-derived benthic temperatures for intermediate (GC528, 598m; blue) and deep waters (MD07-3076, 3770m; black) from the subantarctic South Atlantic (Roberts et al., 2016).

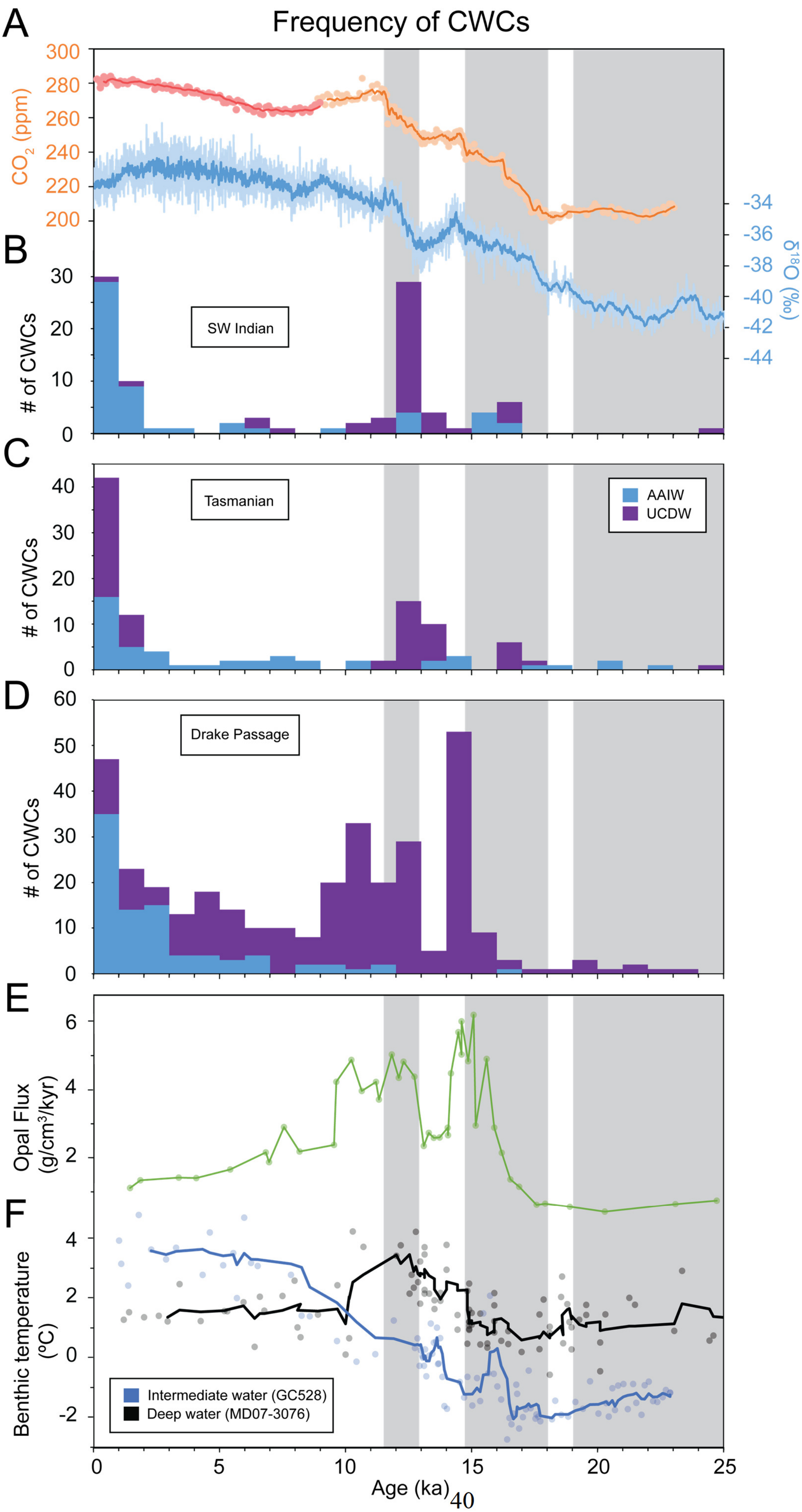
A
Frequency of CWCs
CO2 (ppm)
δ18O (‰)
B
# of CWCs
SW Indian
C
Tasmanian
AAIW
UCDW
D
Drake Passage
E
Opal Flux (g/cm3/kyr)
F
Benthic temperature (°C)
Intermediate water (GC528)
Deep water (MD07-3076)
Age (ka)

4.2.4 The Holocene

Specimens from the early- to mid-Holocene are notably scarce in the SWIO collection, with only seven specimens dating to between 5 and 10 ka, all collected from south of the STF (Figs. 5, 6A). Those that were found are poorly preserved (Fig. 4), possibly indicating greater susceptibility to degradation. During this time interval, deep water carbonate ion concentrations reached their lowest values (Yu et al., 2010). It is possible that a shoaled ASH reduced the suitability of UCDW, whilst the temperature of AAIW was still sub-optimal for coral growth (Fig. 7E; Roberts et al., 2016). Corals are present throughout this period in the Tasmanian and Drake Passage collections (Fig. 7B, C), but at much lower abundances than during the ACR (Margolin et al., 2014; Thiagarajan et al., 2013).

After this decrease in abundance, the number of CWC specimens increases at Coral and Atlantis (Fig. 6). Late Holocene CWC specimens are found at shallower depths compared to the deglacial period, with 95 % of CWC dated to < 6 ka being found in SAMW or AAIW (Fig. 7A). Only two specimens dated to < 6 ka are found below 750 m at Coral Seamount, within UCDW depths, and no live corals were seen below 700 m during ROV surveys (Rogers and Taylor, 2011). In the southeast Pacific (Cape Horn) and Drake Passage (Burdwood Bank), Late Holocene corals are also more common above 1000 m (Margolin et al., 2014; Fig. 7C). South of Tasmania, the CWCs undergo a depth expansion from 2000 to 2400 m in CDW depths, with abundant corals also at shallower AAIW depths, but with a ‘hiatus’ at depths of 1500-1800 m influenced by lower dissolved oxygen values (170-180 μmol/kg; (Thiagarajan et al., 2013).

In the modern subantarctic SWIO, 900-1000 m marks the upper boundary of UCDW, a water mass which brings in old, nutrient-rich deep waters from the northern Indian Ocean and which is associated with a similar dissolved oxygen minimum (< 180 μmol O_2 /kg from 1000

– 1500 m; Figs. 1B, 7) to the Tasmanian coral hiatus (Thiagarajan et al., 2013). The depth of the ASH, controlled mainly by temperature and pressure, is also approximately coincident with UCDW in the region of Coral Seamount (~ 1400 m; Sabine et al., 2002; Fig. 8). Because sampling did not take place below the ASH or oxygen minimum, it is difficult to evaluate their relative influence. However, the coincidence of most late Holocene CWCs between 600 and 800 m with the oxygen peak within AAIW (~220 μmol/kg) is striking.

The absence of CWCs from Atlantis Bank before the late Holocene (Fig. 6A) is difficult to explain in terms of any of the above discussed environmental factors, and may instead be an artefact of the limited depth survey performed there. Today, surface waters at Atlantis Bank have the lowest chlorophyll fluorescence of the four seamounts (Djurhuus et al., 2017b), indicating low productivity and a limited food source, although modern corals there may benefit from organic matter export via SAMW. If anything, food supply at Atlantis Bank is likely to have been higher in the past as a result of increased iron fertilisation (Kohfeld et al., 2005) and a northward-shifted STF (De Deckker et al., 2012; Sikes et al., 2009), making food supply an unlikely factor in controlling their absence. Similarly, temperatures were likely no warmer and oxygen concentrations similar throughout the Holocene at these depths. However, it could perhaps be the case that favourable calcification conditions arose only in the late Holocene, because the ASH shoals to the north in the modern day SWIO (Sabine et al., 2002), making this location particularly sensitive to changes in ocean carbonate chemistry.

Figure 8: Depths and ages (lower axis) of Late Holocene corals at Coral Seamount, colour coded by taxonomic grouping where red dots are Dendrophylliidae and purple dots are *Desmophyllum dianthus*. Precise ages are given for samples which underwent isotope dilution U-series dating, and laser ablation ages are used for all other samples (see Appendices 1-3). Blue curves show seawater oxygen concentration from CTD data at Coral Seamount (upper axis) and the approximate depth of the aragonite saturation horizon (ASH; Sabine et al., 2002) is indicated in orange. Modern day boundaries between Subantarctic Mode Water (SAMW), Antarctic Intermediate Water (AAIW) and Upper Circumpolar Deep Water (UCDW) are indicated with black lines.

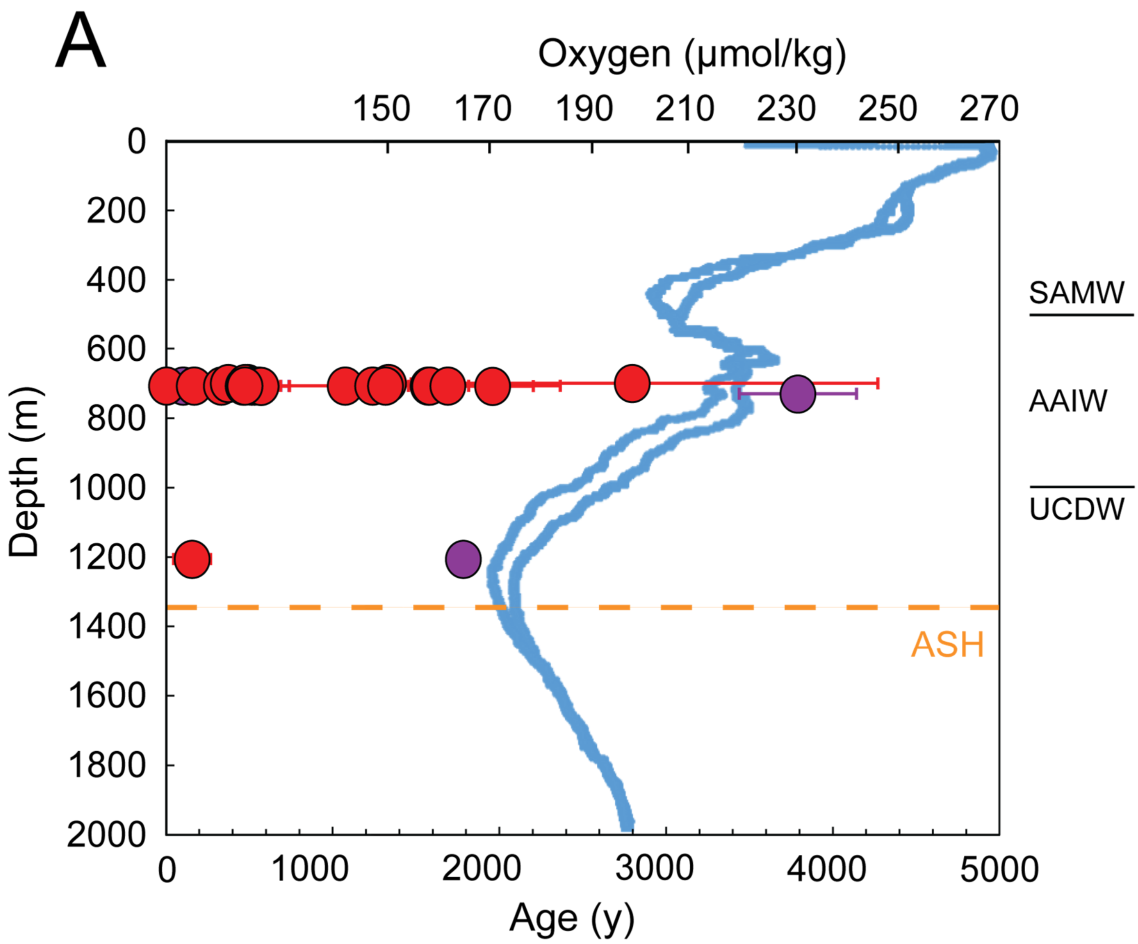

5. Conclusions

The species assemblage of subfossil scleractinian corals recovered from SWIO seamounts indicates influences from the Indian, Pacific, and Antarctic biogeographic zones. Particular diversity and abundance of CWCs at Coral Seamount may be a result of its location in the SAZ, between the Antarctic and Indian biogeographic zones, and higher food availability. We also find indications of biogeographic controls on morphology across the seamount transect, with a more robust *D. dianthus* and *C. diomedeae* morphology occurring more commonly north of the STF, compared to specimens from intermediate and deep waters in the SAZ.

Striking similarities in the temporal distribution of CWCs from the SWIO with other Southern Ocean CWC collections hint at widespread impacts on coral habitats from deglacial changes in ocean stratification and biogeochemistry. As observed elsewhere in the subpolar Southern Ocean, solitary coral growth seems to have been limited during the LGM. Unfavourable carbonate, temperature, and oxygen conditions may have outweighed higher productivity in the SAZ. Although CWCs begin to appear during HS1, we argue that carbonate and oxygen conditions did not become optimal until the late deglacial (14 -11.5 ka), when a peak in abundance is seen in solitary CWC records from the SWIO, Tasmania, and the Drake Passage. This abundance peak is coincident with increased productivity in the Antarctic Zone, which could have provided enhanced supply of POC to the SAZ sites via advection. Water temperatures within AAIW may have been below the habitable range, a possible explanation for the relative lack of solitary CWCs at intermediate depths at this time. In contrast, warmer temperatures within UCDW, combined with greater oxygenation, higher deep-water carbonate ion concentrations and a deeper ASH than during the LGM, could have facilitated colonisation at UCDW depths.

In the late Holocene SAZ, the mid-depth oxygen minimum associated with the inflow of old deep waters from the Indian and Pacific Oceans appears to have been a less favourable habitat for solitary CWCs in the SWIO and Tasmania than well-oxygenated AAIW depths. This observation suggests that their survival here requires higher oxygen concentrations than cold-water coral reefs elsewhere. Future investigations on larger numbers of CWCs, collected in a systematic survey of this region, combined with a greater understanding of the responses of solitary CWC to environmental conditions, would likely provide stronger constraints on the patterns we describe, and on future responses of CWCs to environmental change.

Acknowledgements

The JC066 RRS James Cook expedition was supported by the Global Environment Facility Grant through UNDP Project ID GEF3138/PIMS3657, the IUCN Seamounts Project FFEM-SWIO-P00917, and NERC Grant NE/F005504/1 Benthic Biodiversity of Seamounts in the Southwest Indian Ocean. We thank the science teams and crews of expedition JC066 for collecting the coral samples, and Anni Djurhuus for sharing cruise data. We acknowledge NERC funding to NP through the Science and Solutions for a Changing Planet DTP (NE/L002515/1), TvdF and DJW (NE/N001141/1), SHL (NERC fellowship, NE/P018181/1), NS (NERC NE/R011044/1) and LR (NE/N003861/1). SHL also acknowledges support from a Leverhulme Trust fellowship (ECF-2014-615), and LR from the European Research Council (278705). We are grateful for technical and lab support from Katharina Kreissig, Barry Coles and Carolyn Taylor, and thank Ken Johnson for supervision at the Natural History Museum. We also thank Igor Belkin for editorial handling and Andres Rüggeberg, Jean-Carlos Montero-Serrano and two anonymous reviewers for constructive comments on the manuscript.

References

Addamo, A.M., Martínez-Baraldés, I., Vertino, A., López-González, P.J., Taviani, M., Machordom, A., 2015. Morphological polymorphism of *Desmophyllum dianthus* (Anthozoa: Hexacorallia) over a wide ecological and biogeographic range: Stability in deep habitats? Zool. Anz. 259, 113–130. https://doi.org/10.1016/j.jcz.2015.10.004

Adkins, J.F., McIntyre, K., Schrag, D.P., 2002. The salinity, temperature, and $\delta^{18}O$ of the glacial deep ocean. Science 298, 1769–1773.

Alcock, A., 1902. Report on the deep-sea Madreporaria of the Siboga-Expedition. E. J. Brill, Leiden.

Anderson, B.E., Ali, S., Bradtmiller, L.I., Nielsen, S.H.H., Fleisher, M.Q., Anderson, B.E., Burckle, L.H., 2009. Wind-driven upwelling in the Southern Ocean and the deglacial rise in atmospheric CO_2. Science 323, 1443–1448.

Baco, A.R., Morgan, N., Roark, E.B., Silva, M., Shamberger, K.E.F., Miller, K., 2017. Defying dissolution: Discovery of deep-sea scleractinian coral reefs in the North Pacific. Sci. Rep. 7, 5436. https://doi.org/10.1038/s41598-017-05492-w

Bard, E., Rickaby, R.E.M., 2009. Migration of the subtropical front as a modulator of glacial climate. Nature 460, 380–383. https://doi.org/10.1038/nature08189

Barker, S., Diz, P., Vautravers, M.J., Pike, J., Knorr, G., Hall, I.R., Broecker, W.S., Diz, P., Knorr, G., 2009. Interhemispheric Atlantic seesaw response during the last deglaciation. Nature 457, 1097–1102. https://doi.org/10.1038/nature07770

Beal, L.M., De Ruijter, W.P.M., Biastoch, A., Zahn, R., Cronin, M., Hermes, J., Lutjeharms, J., Quartly, G., Tozuka, T., Baker-Yeboah, S., Bornman, T., Cipollini, P., Dijkstra, H., Hall, I., Park, W., Peeters, F., Penven, P., Ridderinkhof, H., Zinke, J., 2011. On the role of the Agulhas system in ocean circulation and climate. Nature 472, 429–436. https://doi.org/10.1038/nature09983

Belkin, I.M., Gordon, A.L., 1996. Southern Ocean fronts from the Greenwich meridian to Tasmania. J. Geophys. Res. 101, 3675–3696. https://doi.org/10.1029/95JC02750

Bourne, G.C., 1905. Report on the solitary corals collected by Professor Herdman, at Ceylon, in 1902. Rep. to Gov. Ceylon Pearl Oyster Fish. Gulf Manaar 4, 187–211.

Bryan, S.P., Marchitto, T.M., Lehman, S.J., 2010. The release of ^{14}C-depleted carbon from the deep ocean during the last deglaciation: Evidence from the Arabian Sea. Earth Planet. Sci. Lett. 298, 244–254. https://doi.org/10.1016/j.epsl.2010.08.025

Burke, A., Robinson, L.F., 2012. The Southern Ocean's role in carbon exchange during the last deglaciation. Science 335, 557–561. https://doi.org/10.1126/science.1208163

Burke, A., Robinson, L.F., McNichol, A.P., Jenkins, W.J., Scanlon, K.M., Gerlach, D.S., 2010. Reconnaissance dating: A new radiocarbon method applied to assessing the temporal distribution of Southern Ocean deep-sea corals. Deep. Res. Part I Oceanogr. Res. Pap. 57, 1510–1520. https://doi.org/10.1016/j.dsr.2010.07.010

Burke, A., Stewart, A.L., Adkins, J.F., Ferrari, R., Jansen, M.F., Thompson, A.F., 2015. The glacial mid-depth radiocarbon bulge and its implications for the overturning circulation. Paleoceanography 1021–1039. https://doi.org/10.1002/2015PA002778.Received

Büscher, J. V., Form, A.U., Riebesell, U., 2017. Interactive effects of ocean acidification and warming on growth, fitness and survival of the cold-water coral *Lophelia pertusa* under different food availabilities. Front. Mar. Sci. 4, 1–14. https://doi.org/10.3389/fmars.2017.00101

Cairns, S.D., 2007. Deep water corals : an overview with special reference to diversity and distribution of deep-water scleractininan corals. Bull. Mar. Sci. 81, 311–322.

Cairns, S.D., 2000. A revision of the shallow-water azooxanthellate Scleractinia of the western Atlantic. Stud. Nat. Hist. Carribean Reg. 75, 1–215.

Cairns, S.D., 1995. The marine fauna of New Zealand: Scleractinia (Cnidaria Anthozoa). New Zeal. Oceanogr. Inst. Mem. 103, 210. https://doi.org/10.1017/CBO9781107415324.004

Cairns, S.D., 1982. Antarctic and Subantarctic Scleractinia. Biol. Antarct. Seas XI Antarct. Res. Ser. 34, 1–74.

Cairns, S.D., Keller, N.B., 1993. New taxa distributional records of azooxanthellate Scleractinia (Cnidaria, Anthozoa) from the tropical southwest Indian Ocean, with comments on their zoogeography and ecology. Ann. South African Museum 103, 213–292.

Cairns, S.D., Polonio, V., 2013. New records of deep-water Scleractinia off Argentina and the Falkland Islands. Zootaxa 3691, 58–86. https://doi.org/10.11646/zootaxa.3691.1.2

Cairns, S.D., Zibrowius, H., 1997. Cnidaria Anthozoa : azooxanthellate Scleractinia from the Philippine and Indonesian regions. Mem. du Museum Natl. d'Histoire Nat. 172, 27–243.

Chen, T., Robinson, L.F., Burke, A., Southon, J., Spooner, P., Morris, P.J., Ng, H.C., 2015a. Synchronous centennial abrupt events in the ocean and atmosphere during the last deglaciation. Science 349, 1537–1542. https://doi.org/10.1126/science.aac6159

Cheng, H., Adkins, J., Edwards, R.L., Boyle, E.A., 2000a. U-Th dating of deep-sea corals. Geochim. Cosmochim. Acta 64, 2401–2416.

Cheng, H., Adkins, J., Edwards, R.L.L., Boyle, E.A., 2000b. U-Th dating of deep-sea corals. Geochim. Cosmochim. Acta 64, 2401–2416. https://doi.org/10.1016/S0016-

7037(99)00422-6

Crocket, K.C., Lambelet, M., van de Flierdt, T., Rehkämper, M., Robinson, L.F., 2014. Measurement of fossil deep-sea coral Nd isotopic compositions and concentrations by TIMS as NdO+, with evaluation of cleaning protocols. Chem. Geol. 374–375, 128–140. https://doi.org/10.1016/j.chemgeo.2014.03.011

Dana, J.D., 1846. Structure and Classification of Zoophytes. Lea and Blanchard, Philadelphia.

Davies, A.J., Guinotte, J.M., 2011. Global habitat suitability for framework-forming cold-water corals. PLoS One 6, e18483. https://doi.org/10.1371/journal.pone.0018483

De Deckker, P., Moros, M., Perner, K., Jansen, E., 2012. Influence of the tropics and southern westerlies on glacial interhemispheric asymmetry. Nat. Geosci. 5, 266–269. https://doi.org/10.1038/ngeo1431

de Pourtalès, L.F., 1878. Reports on the results of dredging, under the supervision of Alexander Agassiz, in the Gulf of Mexico, by the United States Coast Survey Steamer “Blake”: Corals. Bull. Museum Comp. Zool. 5, 197–212.

de Pourtalès, L.F., 1871. Deep-sea corals, in: Illustrated Catalogue of the Museum of Comparative Zoology. p. 93.

Dezileau, L., Reyss, J.L., Lemoine, F., 2003. Late Quaternary changes in biogenic opal fluxes in the Southern Indian Ocean. Mar. Geol. 202, 143–158. https://doi.org/10.1016/S0025-3227(03)00283-4

Djurhuus, A., Boersch-Supan, P.H., Mikalsen, S.O., Rogers, A.D., 2017a. Microbe biogeography tracks water masses in a dynamic oceanic frontal system. R. Soc. Open Sci. 4, 170033. https://doi.org/10.1098/rsos.170033

Djurhuus, A., Read, J.F., Rogers, A.. D., 2017b. The spatial distribution of particulate organic carbon and microorganisms on seamounts of the South West Indian Ridge. Deep. Res. Part II Top. Stud. Oceanogr. 136, 73–84. https://doi.org/10.1016/j.dsr2.2015.11.015

Dodds, L.A., Roberts, J.M., Taylor, A.C., Marubini, F., 2007. Metabolic tolerance of the cold-water coral *Lophelia pertusa* (Scleractinia) to temperature and dissolved oxygen change. J. Exp. Mar. Bio. Ecol. 349, 205–214. https://doi.org/10.1016/j.jembe.2007.05.013

Douville, E., Sallé, E., Frank, N., Eisele, M., Pons-Branchu, E., Ayrault, S., 2010. Rapid and accurate U-Th dating of ancient carbonates using inductively coupled plasma-quadrupole mass spectrometry. Chem. Geol. 272, 1–11. https://doi.org/10.1016/j.chemgeo.2010.01.007

Dueñas, L.F., Tracey, D.M., Crawford, A.J., Wilke, T., Alderslade, P., Sánchez, J.A., 2016. The Antarctic Circumpolar Current as a diversification trigger for deep-sea octocorals. BMC Evol. Biol. 16, 2. https://doi.org/10.1186/s12862-015-0574-z

Duineveld, G.C.A., Lavaleye, M.S.S., Bergman, M.J.N., De Stigter, H., Mienis, F., 2007. Trophic structure of a cold-water coral mound community (Rockall Bank, NE Atlantic) in relation to the near-bottom particle supply and current regime. Bull. Mar. Sci. 81, 449–467.

Dullo, W.C., Flögel, S., Rüggeberg, A., 2008. Cold-water coral growth in relation to the hydrography of the Celtic and Nordic European continental margin. Mar. Ecol. Prog. Ser. 371, 165–176. https://doi.org/10.3354/meps07623

Duncan, P.M., 1873. A description of the Madreporaria dredged up during the expeditions of H.M.S. “Porcupine” in 1869 and 1870. Part I. Trans. Zool. Soc. London 8, 303–344. https://doi.org/10.1111/j.1096-3642.1873.tb00560.x

Durand, A., Chase, Z., Noble, T.L., Bostock, H., Jaccard, S.L., Townsend, A.T., Bindoff, N.L., Neil, H., Jacobsen, G., 2018. Reduced oxygenation at intermediate depths of the southwest Pacific during the last glacial maximum. Earth Planet. Sci. Lett. 491, 48–57. https://doi.org/10.1016/j.epsl.2018.03.036

Elmore, A.C., McClymont, E.L., Elderfield, H., Kender, S., Cook, M.R., Leng, M.J., Greaves, M., Misra, S., 2015. Antarctic Intermediate Water properties since 400 ka recorded in infaunal (*Uvigerina peregrina*) and epifaunal (*Planulina wuellerstorfi*) benthic foraminifera. Earth Planet. Sci. Lett. 428, 193–203. https://doi.org/10.1016/j.epsl.2015.07.013

Esper, E.J.C., 1794. Die Pflanzenthiere in Abbildungen nach der Natur mit Farben erleuchtet nebst Beschreibungen. Raspeschen Buchhandlung, Nürnberg.

Ferrari, R., Jansen, M.F., Adkins, J.F., Burke, A., Stewart, A.L., Thompson, A.F., Ferrari, R., Jansen, M.F., Adkins, J.F., Burke, A., Thompson, A.F., 2014. Antarctic sea ice control on ocean circulation in present and glacial climates. Proc. Natl. Acad. Sci. 111, 8753–8758. https://doi.org/10.1073/pnas.1323922111

Fink, H.G., Wienberg, C., Hebbeln, D., McGregor, H. V., Schmiedl, G., Taviani, M., Freiwald, A., 2012. Oxygen control on Holocene cold-water coral development in the eastern Mediterranean Sea. Deep. Res. Part I Oceanogr. Res. Pap. 62, 89–96. https://doi.org/10.1016/j.dsr.2011.12.013

Franzese, A.M., Hemming, S.R., Goldstein, S.L., Anderson, R.F., 2006. Reduced Agulhas Leakage during the Last Glacial Maximum inferred from an integrated provenance and flux study. Earth Planet. Sci. Lett. 250, 72–88. https://doi.org/10.1016/j.epsl.2006.07.002

Gori, A., Ferrier-Pagès, C., Hennige, S.J., Murray, F., Rottier, C., Wicks, L.C., Roberts, J.M.,

2016. Physiological response of the cold-water coral Desmophyllum dianthus to thermal stress and ocean acidification. PeerJ 2016, e1606. https://doi.org/10.7717/peerj.1606

Gravier, C., 1914. Sur une espèce nouvelle de Madréporaire (Desmophyllum antarcticum). Bull. Muséum Hist. Nat. Paris 20, 236–238.

Gray, J.E., 1847. An outline of an arrangement of stony corals. Ann. Mag. Nat. Hist. Ser. 1 19, 120–128.

Guinotte, J.M., Orr, J., Cairns, S., Freiwald, A., Morgan, L., George, R., 2006. Will human-induced changes in seawater chemistry alter the distribution of deep-sea scleractinian corals? Front. Ecol. Environ. 4, 141–146. https://doi.org/10.1890/1540-9295(2006)004[0141:WHCISC]2.0.CO;2

Henry, L.A., Frank, N., Hebbeln, D., Wienberg, C., Robinson, L.F., van de Flierdt, T., Dahl, M., Douarin, M., Morrison, C.L., Correa, M.L., Rogers, A.D., Ruckelshausen, M., Roberts, J.M., 2014. Global ocean conveyor lowers extinction risk in the deep sea. Deep. Res. Part I Oceanogr. Res. Pap. 88, 8–16. https://doi.org/10.1016/j.dsr.2014.03.004

Hines, S.K. V, Southon, J.R., Adkins, J.F., 2015. A high-resolution record of Southern Ocean intermediate water radiocarbon over the past 30,000 years. Earth Planet. Sci. Lett. 432, 46–58. https://doi.org/10.1016/j.epsl.2015.09.038

Jaccard, S.L., Galbraith, E.D., 2012. Large climate-driven changes of oceanic oxygen concentrations during the last deglaciation. Nat. Geosci. 5, 151–156. https://doi.org/10.1038/ngeo1352

Jaccard, S.L., Galbraith, E.D., Martínez-García, A., Anderson, R.F., 2016. Covariation of deep Southern Ocean oxygenation and atmospheric CO_2 through the last ice age. Nature 530, 207–10. https://doi.org/10.1038/nature16514

Kaufman, A., Broecker, W., 1965. Comparison of ^{230}Th and ^{14}C ages for carbonate materials from lakes Lahontan and Bonneville. J. Geophys. Res. 70, 4039–4054.

Keller, N.B., 1976. The deep-sea madreporarian corals of the genus *Fungiacyathus* from the Kurile-Kamchatka, Aleutian Trenches and other regions of the world oceans. Tr. Inst. Okeanol. 99, 31–44.

Kitahara, M. V., Cairns, S.D., Miller, D.J., 2010. Monophyletic origin of Caryophyllia (Scleractinia, Caryophylliidae), with descriptions of six new species. Syst. Biodivers. 8, 91–118. https://doi.org/10.1080/14772000903571088

Kohfeld, K.E., Chase, Z., 2017. Temporal evolution of mechanisms controlling ocean carbon uptake during the last glacial cycle. Earth Planet. Sci. Lett. 472, 206–215. https://doi.org/10.1016/j.epsl.2017.05.015

Kohfeld, K.E., Harrison, S.P., Que, C. Le, Anderson, R.F., 2005. Role of marine biology in glacial-interglacial CO_2 cycles. Science 308, 74–78. https://doi.org/10.1126/science.1105375

Labracherie, M., Labeyrie, L.D., Duprat, J., Bard, E., Arnold, M., Pichon, J.-J., Duplessy, J.C., 1989. The last deglaciation in the Southern Ocean. Paleoceanography 4, 629–638. https://doi.org/10.1029/PA004i006p00629

Linnaeus, C., 1758. Systema naturæ per regna tria naturæ, secundum classes, ordines, genera, species, cum characteribus, differentiis, synonymis, locis. Tomus I. Laurentii Salvii, Holmiæ.

Lomitschka, M., Mangini, A., 1999. Precise Th/U-dating of small and heavily coated samples of deep sea corals. Earth Planet. Sci. Lett. 170, 391–401. https://doi.org/10.1016/S0012-821X(99)00117-X

Lutjeharms, J.R.E., Van Ballegooyen, R.C., 1988. The retroflection of the Aghulas Current. J. Phys. Oceanogr. 18, 1570–1583.

Mangini, A., Godoy, J.M., Godoy, M.L., Kowsmann, R., Santos, G.M., Ruckelshausen, M., Schroeder-Ritzrau, A., Wacker, L., 2010. Deep sea corals off Brazil verify a poorly ventilated Southern Pacific Ocean during H2, H1 and the Younger Dryas. Earth Planet. Sci. Lett. 293, 269–276. https://doi.org/10.1016/j.epsl.2010.02.041

Marcott, S.A., Bauska, T.K., Buizert, C., Steig, E.J., Rosen, J.L., Cuffey, K.M., Fudge, T.J., Severinghaus, J.P., Ahn, J., Kalk, M.L., McConnell, J.R., Sowers, T., Taylor, K.C., White, J.W.C., Brook, E.J., 2014. Centennial-scale changes in the global carbon cycle during the last deglaciation. Nature 514, 616–9. https://doi.org/10.1038/nature13799

Marenzeller, E.V., 1904. Reports on dredging operations of the west coast of central America and Galapagos by the U.S. Fish Commission Steamer 'Albatross' during 1891: Steinkorallen und Hydro-Korallen. Bull. Museum Comp. Zool. 43, 75–87.

Margolin, A.R., Robinson, L.F., Burke, A., Waller, R.G., Scanlon, K.M., Roberts, M.L., Auro, M.E., van de Flierdt, T., 2014. Temporal and spatial distributions of cold-water corals in the Drake Passage: Insights from the last 35,000 years. Deep. Res. Part II Top. Stud. Oceanogr. 99, 237–248. https://doi.org/10.1016/j.dsr2.2013.06.008

Marshall, J., Speer, K., 2012. Closure of the meridional overturning circulation through Southern Ocean upwelling. Nat. Geosci. 5, 171–180. https://doi.org/10.1038/ngeo1391

Martínez-Botí, M.A., Marino, G., Foster, G.L., Ziveri, P., Henehan, M.J., Rae, J.W.B., Mortyn, P.G., Vance, D., Marino, G., Ziveri, P., Henehan, M.J., Foster, G.L., Vance, D., Martínez-Botí, M.A., Rae, J.W.B., 2015. Boron isotope evidence for oceanic carbon dioxide leakage during the last deglaciation. Nature 518, 219–222. https://doi.org/10.1038/nature14155

Martínez-García, A., Sigman, D.M., Ren, H., Anderson, R.F., Straub, M., Hodell, D.A., Jaccard, S.L., Eglinton, T.I., Haug, G.H., 2014. Iron fertilization of the Subantarctic ocean during the last ice age. Science 343, 1347–50. https://doi.org/10.1126/science.1246848

Mastumoto, K., Lynch-Stieglitz, J., Anderson, R.F., 2001. Similar glacial and Holocene Southern Ocean hydrography. Paleoceanography 16, 445–454.

McCave, I.N., Crowhurst, S.J., Kuhn, G., Hillenbrand, C.D., Meredith, M.P., 2014. Minimal change in Antarctic Circumpolar Current flow speed between the last glacial and Holocene. Nat. Geosci. 7, 113–116. https://doi.org/10.1038/ngeo2037

McCave, I.N., Kiefer, T., Thornalley, D.J.R., Elderfield, H., 2005. Deep flow in the Madagascar-Mascarene Basin over the last 150 000 years. Philos. Trans. R. Soc. A Math. Phys. Eng. Sci. 363, 81–99. https://doi.org/10.1098/rsta.2004.1480

Miller, K.J., Rowden, A.A., Williams, A., Haussermann, V., 2011. Out of their depth? isolated deep populations of the cosmopolitan coral *Desmophyllum dianthus* may be highly vulnerable to environmental change. PLoS One 6. https://doi.org/10.1371/journal.pone.0019004

Milne Edwards, H., Haime, J., 1848. Recherches sur les polypiers. Deuxième mémoire. Monographie des turbinolides. Ann. des Sci. Nat. série 3, Zool. 9, 211–344, pl. 7–10.

Monnin, E., Indermühle, A., Dällenbach, A., Flückiger, J., Stauffer, B., Stocker, T.F., Raynaud, D., Barnola, J.-M., 2001. Atmospheric CO_2 concentrations over the Last Glacial Termination. Science 291, 112–114. https://doi.org/10.1126/science.291.5501.112

Montero-Serrano, J.-C., Frank, N., Tisnérat-Laborde, N., Colin, C., Wu, C.-C., Lin, K., Shen, C.-C., Copard, K., Orejas, C., Gori, A., De Mol, L., Van Rooij, D., Reverdin, G., Douville, E., 2013. Decadal changes in the mid-depth water mass dynamic of the Northeastern Atlantic margin (Bay of Biscay). Earth Planet. Sci. Lett. 364, 134–144. https://doi.org/10.1016/j.epsl.2013.01.012

Moseley, H.N., 1881. Report on Certain Hydroid, Alcyonarian, and Madreporarian Corals Procured during the Voyage of H. M. S. Challenger, in the Years 1873-1876. Zoology 2, 1–248.

Naumann, M.S., Orejas, C., Wild, C., Ferrier-Pages, C., 2011. First evidence for zooplankton feeding sustaining key physiological processes in a scleractinian cold-water coral. J. Exp. Biol. 214, 3570–3576. https://doi.org/10.1242/jeb.061390

Ninnemann, U.S., Charles, C.D., 2002. Changes in the mode of Southern Ocean circulation over the last glacial cycle revealed by foraminiferal stable isotopic variability. Earth Planet. Sci. Lett. 201, 383–396. https://doi.org/10.1016/S0012-821X(02)00708-2

Parrenin, F., Masson-Delmotte, V., Köhler, P., Raynaud, D., Paillard, D., Schwander, J., Barbante, C., Landais, A., Wegner, A., Jouzel, J., Kohler, P., Raynaud, D., Paillard, D., Schwander, J., Barbante, C., Landais, A., Wegner, A., Jouzel, J., 2013. Synchronous change of atmospheric CO_2 and Antarctic temperature during the last deglacial warming. Science 339, 1060–1063. https://doi.org/10.1126/science.1226368

Plancherel, Y., 2012. A study of the ocean’s water masses using data and models. Princeton University.

Pollard, R.T., Venables, H.J., Read, J.F., Allen, J.T., 2007. Large-scale circulation around the Crozet Plateau controls an annual phytoplankton bloom in the Crozet Basin. Deep. Res. Part II Top. Stud. Oceanogr. 54, 1915–1929. https://doi.org/10.1016/j.dsr2.2007.06.012

Rae, J.W., Burke, A., Robinson, L.F., Adkins, J.F., Chen, T., Cole, C., Greenop, R., Li, T., Littley, E., Nita, D.C., Stewart, J.A., Taylor, B., 2018. CO_2 storage and release in the deep Southern Ocean on millennial to centennial timescales. Nature 562, 569–573. https://doi.org/10.1038/s41586-018-0614-0

Read, J.F., Lucas, M.I., Holley, S.E., Pollard, R.T., 2000. Phytoplankton, nutrients and hydrography in the frontal zone between the Southwest Indian Subtropical gyre and the Southern Ocean. Deep. Res. Part I Oceanogr. Res. Pap. 47, 2341–2368. https://doi.org/10.1016/S0967-0637(00)00021-2

Read, J.F., Pollard, R., 2017. An introduction to the physical oceanography of six seamounts in the southwest Indian Ocean. Deep. Res. Part II Top. Stud. Oceanogr. 136, 44–58. https://doi.org/10.1016/j.dsr2.2015.06.022

Reimer, P.J., Baille, M.G.L., Bard, E., Bayliss, A., Beck, J.W., Blackwell, P.G., Bronk Ramsey, C., Buck, C.E., Burr, G.S., 2009. INTCAL09 and MARINE09 radiocarbon age calibration curves, 0-50,000 years cal BP. Radiocarbon 51, 1111–1150.

Roberts, J., Gottschalk, J., Skinner, L.C., Peck, V.L., Kender, S., Elderfield, H., Waelbroeck, C., Vázquez Riveiros, N., Hodell, D.A., Gottschalk, J., Elderfield, H., Peck, V.L., Skinner, L.C., Kender, S., Hodell, D.A., Roberts, J., Vázquez Riveiros, N., 2016. Evolution of South Atlantic density and chemical stratification across the last deglaciation. Proc. Natl. Acad. Sci. 113, 514–519. https://doi.org/10.1073/pnas.1511252113

Roberts, J., McCave, I.N., McClymont, E.L., Kender, S., Hillenbrand, C.D., Matano, R., Hodell, D.A., Peck, V.L., 2017. Deglacial changes in flow and frontal structure through the Drake Passage. Earth Planet. Sci. Lett. 474, 397–408. https://doi.org/10.1016/j.epsl.2017.07.004

Roberts, J.M., Wheeler, A.J., Freiwald, A., 2006. Reefs of the deep: the biology and geology of cold-water coral ecosystems. Science 312, 543–7. https://doi.org/DOI

10.1126/science.1119861

Roberts, J.M., Wheeler, A.J., Friewald, A., Cairns, S.D., 2009. Cold-Water Corals: The Biology and Geology of Deep-Sea Coral Habitats. Cambridge University Press, Cambridge.

Robinson, L.F., Adkins, J.F., Frank, N., Gagnon, A.C., Prouty, N.G., Brendan Roark, E., van de Flierdt, T., 2014. The geochemistry of deep-sea coral skeletons: A review of vital effects and applications for palaeoceanography. Deep. Res. Part II Top. Stud. Oceanogr. 99, 184–198. https://doi.org/10.1016/j.dsr2.2013.06.005

Rogers, A.D., Taylor, M.L., 2011. Benthic biodiversity of seamounts in the southwest Indian Ocean: Cruise Report – R/V James Cook 066 Southwest Indian Ocean Seamounts expedition.

Romahn, S., MacKensen, A., Groeneveld, J., Pätzold, J., 2014. Deglacial intermediate water reorganization: New evidence from the Indian Ocean. Clim. Past 10, 293–303. https://doi.org/10.5194/cp-10-293-2014

Sabine, C.L., Key, R.M., Feely, R.A., Greeley, D., 2002. Inorganic carbon in the Indian Ocean: Distribution and dissolution processes. Global Biogeochem. Cycles 16, 15-1-15–18. https://doi.org/10.1029/2002GB001869

Schlitzer, R., 2017. Ocean Data View [WWW Document]. URL odv.awi.de

Shen, C.-C., Li, K.-S., Sieh, K., Natawidjaja, D., Cheng, H., Wang, X., Edwards, R.L., Lam, D.D., Hsieh, Y.-T., Fan, T.-Y., Meltzner, A.J., Taylor, F.W., Quinn, T.M., Chiang, H.-W., Kilbourne, K.H., 2008. Variation of initial ^{230}Th/^{232}Th and limits of high precision U–Th dating of shallow-water corals. Geochim. Cosmochim. Acta 72, 4201–4223. https://doi.org/10.1016/j.gca.2008.06.011

Shen, C.-C., Wu, C.-C., Cheng, H., Lawrence Edwards, R., Hsieh, Y.-T., Gallet, S., Chang, C.-C., Li, T.-Y., Lam, D.D., Kano, A., Hori, M., Spötl, C., 2012. High-precision and high-resolution carbonate ^{230}Th dating by MC-ICP-MS with SEM protocols. Geochim. Cosmochim. Acta 99, 71–86. https://doi.org/10.1016/j.gca.2012.09.018

Shen, G.T., Boyle, E.A., 1988. Determination of lead, cadmium and other trace metals in annually-banded corals. Chem. Geol. 67, 47–62. https://doi.org/10.1016/0009-2541(88)90005-8

Siani, G., Michel, E., De Pol-Holz, R., DeVries, T., Lamy, F., Carel, M., Isguder, G., Dewilde, F., Lourantou, A., 2013. Carbon isotope records reveal precise timing of enhanced Southern Ocean upwelling during the last deglaciation. Nat. Commun. 4, 1–9. https://doi.org/10.1038/ncomms3758

Sigman, D.M., Hain, M.P., Haug, G.H., 2010. The polar ocean and glacial cycles in atmospheric CO_2 concentration. Nature 466, 47–55. https://doi.org/10.1038/nature09149

Sikes, E.L., Howard, W.R., Samson, C.R., Mahan, T.S., Robertson, L.G., Volkman, J.K., 2009. Southern Ocean seasonal temperature and Subtropical Front movement on the South Tasman Rise in the late Quaternary. Paleoceanography 24, 1–13. https://doi.org/10.1029/2008PA001659

Skinner, L.C., Fallon, S., Waelbroeck, C., Michel, E., Barker, S., 2010. Ventilation of the deep Southern Ocean and deglacial CO_2 rise. Science 328, 1147–1151. https://doi.org/10.1126/science.1183627

Sokolov, S., Rintoul, S.R., 2009. Circumpolar structure and distribution of the antarctic circumpolar current fronts: 1. Mean circumpolar paths. J. Geophys. Res. Ocean. 114, 1–19. https://doi.org/10.1029/2008JC005108

Spooner, P.T., Chen, T., Robinson, L.F., Coath, C.D., 2016. Rapid uranium-series age screening of carbonates by laser ablation mass spectrometry. Quat. Geochronol. 31, 28–39. https://doi.org/10.1016/j.quageo.2015.10.004

Squires, D.F., 1961. Deep Sea Corals Collected by the Lamont Geological Observatory: Scotia Sea Corals. American Museum of Natural History.

Stanley, G.D., Cairns, S.D., 1988. Constructional azooxanthellate coral communities: An overview with implications for the fossil record. Palaios 3, 233. https://doi.org/10.2307/3514534

Stenni, B., Buiron, D., Frezzotti, M., Albani, S., Barbante, C., Bard, E., Barnola, J.M.M., Baroni, M., Baumgartner, M., Bonazza, M., Capron, E., Castellano, E., Chappellaz, J., Delmonte, B., Falourd, S., Genoni, L., Iacumin, P., Jouzel, J., Kipfstuhl, S., Landais, A., Lemieux-Dudon, B., Maggi, V., Masson-Delmotte, V., Mazzola, C., Minster, B., Montagnat, M., Mulvaney, R., Narcisi, B., Oerter, H., Parrenin, F., Petit, J.R.R., Ritz, C., Scarchilli, C., Schilt, A., Schüpbach, S., Schwander, J., Selmo, E., Severi, M., Stocker, T.F.F., Udisti, R., 2011. Expression of the bipolar see-saw in Antarctic climate records during the last deglaciation. Nat. Geosci. 4, 46–49. https://doi.org/10.1038/ngeo1026

Stenni, B., Masson-Delmotte, V., Johnsen, S., Jouzel, J., Longinelli, A., Monnin, E., Röthlisberger, R., Selmo, E., 2001. An oceanic cold reversal during the last deglaciation. Science 293, 2074–2077. https://doi.org/10.1126/science.1059702

Stephens, B.B., Keeling, R.F., 2000. The influence of Antarctic sea ice on glacial-interglacial CO_2 variations. Nature 404, 171–174. https://doi.org/10.1038/35004556

Thiagarajan, N., Gerlach, D., Roberts, M.L., Burke, A., McNichol, A., Jenkins, W.J., Subhas, A. V., Thresher, R.E., Adkins, J.F., 2013. Movement of deep-sea coral populations on climatic timescales. Paleoceanography 28, 227–236. https://doi.org/10.1002/palo.20023

Thresher, R.E., Tilbrook, B., Fallon, S., Wilson, N.C., Adkins, J., 2011. Effects of chronic low carbonate saturation levels on the distribution, growth and skeletal chemistry of deep-sea corals and other seamount megabenthos. Mar. Ecol. Prog. Ser. 442, 87–96. https://doi.org/10.3354/meps09400

van Aken, H.M., Ridderinkhof, H., de Ruijter, W.P.M., 2004. North Atlantic deep water in the south-western Indian Ocean. Deep Sea Res. Part I Oceanogr. Res. Pap. 51, 755–776. https://doi.org/10.1016/j.dsr.2004.01.008

van de Flierdt, T., Robinson, L.F., Adkins, J.F., 2010. Deep-sea coral aragonite as a recorder for the neodymium isotopic composition of seawater. Geochim. Cosmochim. Acta 74, 6014–6032. https://doi.org/10.1016/j.gca.2010.08.001

WAIS Divide Project Members, 2015. Precise interpolar phasing of abrupt climate change during the last ice age. Nature 520, 661–665. https://doi.org/10.1038/nature14401

Wang, X.T., Sigman, D.M., Prokopenko, M.G., Adkins, J.F., Robinson, L.F., Hines, S.K., Chai, J., Studer, A.S., Martínez-García, A., Chen, T., Haug, G.H., 2017. Deep-sea coral evidence for lower Southern Ocean surface nitrate concentrations during the last ice age. Proc. Natl. Acad. Sci. 114, 3352–3357. https://doi.org/10.1073/pnas.1615718114

Watling, L., Guinotte, J., Clark, M.R., Smith, C.R., 2013. A proposed biogeography of the deep ocean floor. Prog. Oceanogr. 111, 91–112. https://doi.org/10.1016/j.pocean.2012.11.003

Yu, J., Broecker, W.S., Elderfield, H., Jin, Z., McManus, J.F., Zhang, F., 2010. Loss of carbon from the deep sea since the Last Glacial Maximum. Science 330, 1084–1087.

Zibrowius, H., 1980. Les scléractiniaires de la Méditerranée et de l’Atlantique nord-oriental. Mémoires de l’Institut Océanographique, Monaco 11, 1–284.

Contributions

All authors have contributed to this work. Their individual roles are detailed as follows: NP carried out sample identifications, prepared samples for dating, interpreted the data, and wrote the manuscript with input from all authors; ADR and MLT carried out sample collection on the JC066 cruise, following the request of TvdF, and assisted with video analysis of sample locations; TC led the laser ablation and isotope dilution U-series dating and data processing, and Tao Li carried out part of the isotope dilution U-series analyses, under the supervision of LFR at the University of Bristol; NS provided training and guidance on taxonomic analysis of the specimens at the Natural History Museum and edits on the manuscript; LFR, TvdF, DJW and SHL aided discussions on data interpretation. All authors edited and have approved the final manuscript.

Conflicts of interest

Declarations of interest: none.

Notes for editor

Please use colour for all figures in print.

Appendices

Appendix 1: Solitary scleractinian samples from JC066 expedition to SWIO seamounts

Cruise	Seamount	Latitude (°N)	Longitude (°E)	Sample number	Depth / m	Family	Genus	Species	Mass / g	Max calicular diameter / cm	Height / cm	LA Age / y	2σ	ID Age / y	2σ
JC066	Coral	-41.3628	42.9151	2812D	709.5	Dendrophylliidae	*Balanophyllia*	*gigas*	0.5	7.9	20.2	0	362		
JC066	Coral	-41.3485	42.9208	1057	1207.2	Dendrophylliidae	*Balanophyllia*	*gigas*	1	10.5	16.3	154	111		
JC066	Coral	-41.3628	42.9151	2812B	709.5	Dendrophylliidae	*Balanophyllia*	*gigas*	0.6	8.7	23.1	166	147		
JC066	Coral	-41.3628	42.9151	2810	709.5	Caryophylliidae	*Desmophyllum*	*dianthus*	4.28	21.2	29.3	327	277	99	17
JC066	Coral	-41.3628	42.9151	2812G	709.5	Dendrophylliidae	*Balanophyllia*	*gigas*	0.4	7.2	17.2	329	155		
JC066	Coral	-41.3628	42.9149	2808	702	Dendrophylliidae	*Balanophyllia*	*gigas*	0.64	9.4	25.6	369	147		
JC066	Coral	-41.3628	42.9151	2812K	709.5	Dendrophylliidae	*Balanophyllia*	*gigas*	0.1	8.6	14.7	460	115		
JC066	Coral	-41.3628	42.9151	2812E	709.5	Dendrophylliidae	*Balanophyllia*	*malouinensis*	0.5	0.7	2.3	471	113		
JC066	Coral	-41.3628	42.9149	2803	702	Dendrophylliidae	*Balanophyllia*	*gigas*	0.54	7.2	21.3	473	133		
JC066	Coral	-41.3628	42.9151	2812Q	709.5	Dendrophylliidae	*Balanophyllia*	*gigas*	0.2	5.8	14.6	511	173		
JC066	Coral	-41.3628	42.9151	2812F	709.5	Caryophylliidae	*Desmophyllum*	*dianthus*	0.5	9.2	22.5	527	208		
JC066	Coral	-41.3628	42.9151	2811	709.5	Caryophylliidae	*Desmophyllum*	*dianthus*	1.4	13.2	33.8	553	134		
JC066	Coral	-41.3627	42.9151	2799	710	Dendrophylliidae	*Balanophyllia*	*gigas*	0.29	8	17	567	171		
JC066	Coral	-41.3628	42.9149	2795	702	Caryophylliidae	*Desmophyllum*	*dianthus*	5.26	20.9	44	609	227	486	128
JC066	Coral	-41.3628	42.9151	2812L	709.5	Dendrophylliidae	*Balanophyllia*	*gigas*	0.9	5.9	20.7	1072	1291		
JC066	Coral	-41.3628	42.9151	2812I	709.5	Dendrophylliidae	*Balanophyllia*	*gigas*	0.5	8	19.7	1237	186		
JC066	Coral	-41.3628	42.9151	2812M	709.5	Dendrophylliidae	*Leptopsammia*	*stokesiana*	0.3	6.8	17.8	1314	139		
JC066	Coral	-41.3628	42.9149	2807	702	Dendrophylliidae	*Balanophyllia*	*gigas*	1.06	8.3	28.4	1332	138		
JC066	Coral	-41.3485	42.9208	0117	1207.2	Caryophylliidae	*Desmophyllum*	*dianthus*	8.7	30.3	18.4	1476	280	1782	48
JC066	Coral	-41.3628	42.9151	2812C	709.5	Dendrophylliidae	*Balanophyllia*	*gigas*	0.8	7.6	21.8	1571	243		
JC066	Coral	-41.3628	42.9151	2812J	709.5	Dendrophylliidae	*Balanophyllia*	*malouinensis*	0.3	0.7	2	1579	175		
JC066	Coral	-41.3628	42.9151	2812V	709.5	Dendrophylliidae	*Leptopsammia*	*stokesiana*	0.05	6.6	13.4	1689	176		
JC066	Coral	-41.3627	42.9151	2799B	710	Dendrophylliidae	*Leptopsammia*	*stokesiana*	0.59	8.1	16.6	1957	245		

JC066	Coral	-41.3628	42.9149	2809	702	Dendrophylliidae	*Leptopsammia*	*stokesiana*	0.52	8	22.4	2796	1474		
JC066	Coral	-41.3725	42.9107	1116	732	Caryophylliidae	*Desmophyllum*	*dianthus*	8.35	28.5	34.4	4058	410	3790	352
JC066	Coral	-41.3724	42.9102	1104B	732	Caryophylliidae	*Trochocyathus*	*gordoni*	0.3	9.2	11.1	5013	326		
JC066	Coral	-41.3724	42.9102	1104A	732	Caryophylliidae	*Trochocyathus*	*gordoni*	0.8	11	10.4	5193	389		
JC066	Coral	-41.3339	42.9188	0486C	1097.2	Flabellidae	*Javania*	*antarctica*	0.7	12.4	19.6	6610	809		
JC066	Coral	-41.3485	42.9208	1062	1207.2	Flabellidae	*Flabellum*	*flexuosum*	0.63	12.3	22.9	6832	333		
JC066	Coral	-41.3485	42.9208	1063	1207.2	Caryophylliidae	*Desmophyllum*	*dianthus*	2.94	16.1	18.6	7176	491		
JC066	Coral	-41.3457	42.9229	0157	1395	Caryophylliidae	*Desmophyllum*	*dianthus*	4.84	20.5	30	9777	1419	11262	242
JC066	Coral	-41.3485	42.9208	1156	1207.2	Caryophylliidae	*Desmophyllum*	*dianthus*	2.27	15.8	31.6	10521	727	10568	290
JC066	Coral	-41.3339	42.9188	1145	1097.2	Caryophylliidae	*Desmophyllum*	*dianthus*	2.86	20.4	28.5	10670	1010		
JC066	Coral	-41.3485	42.9208	1069	1207.2	Flabellidae	*Javania*	*antarctica*	0.74	9.2	23.5	10911	613		
JC066	Coral	-41.3485	42.9208	0125	1207.2	Caryophylliidae	*Caryophyllia*	*diomedeae*	3.1	13.5	25	11975	705	12490	168
JC066	Coral	-41.3485	42.9208	0124	1207.2	Caryophylliidae	*Caryophyllia*	*diomedeae*	6.33	13.2	35.2	12050	709	11941	320
JC066	Coral	-41.3485	42.9208	0128	1207.2	Caryophylliidae	*Desmophyllum*	*dianthus*	3.82	18.3	19.1	12053	1090	12967	68
JC066	Coral	-41.3485	42.9208	1064	1207.2	Dendrophylliidae	*Balanophyllia*	*gigas*	1.12	8.5	20.8	12268	592		
JC066	Coral	-41.3339	42.9188	0486D	1097.2	Flabellidae	*Javania*	*antarctica*	0.5	13	18.5	12289	600		
JC066	Coral	-41.3485	42.9208	1056	1207.2	Caryophylliidae	*Caryophyllia*	*diomedeae*	7	20.3	44.3	12339	615	12307	985
JC066	Coral	-41.3628	42.9151	2812R	709.5	Dendrophylliidae	*Balanophyllia*	*malouinensis*	0.5	1.1	2	12395	522		
JC066	Coral	-41.3485	42.9208	0120	1207.2	Flabellidae	*Flabellum*	*flexuosum*	0.72	11.2	20.2	12418	622		
JC066	Coral	-41.3485	42.9208	1160	1207.2	Caryophylliidae	*Desmophyllum*	*dianthus*	1.64	15.5	22.9	12635	789	13195	82
JC066	Coral	-41.3485	42.9208	1059	1207.2	Caryophylliidae	*Desmophyllum*	*dianthus*	1.47	fragmentary	fragmentary	12744	607		
JC066	Coral	-41.3724	42.9102	1072	*624*	Caryophylliidae	*?*	*?*	0.59			12762	665		
JC066	Coral	-41.3485	42.9208	1155	1207.2	Caryophylliidae	*Caryophyllia*	*diomedeae*	2.2	11	27.5	12767	629	12435	134
JC066	Coral	-41.3485	42.9208	1066B	1207.2	Caryophylliidae	*Desmophyllum*	*dianthus*	3.96	17.7	39	12818	792	12939	185
JC066	Coral	-41.3485	42.9208	0119	1207.2	Caryophylliidae	*Dasmosmilia*	*lymani*	0.37	8.5	16.1	12818	600		
JC066	Coral	-41.3485	42.9208	0126B	1207.2	Caryophylliidae	*Caryophyllia*	*diomedeae*	1.86	10.7	22.3	12930	649	12702	218
JC066	Coral	-41.3485	42.9208	0118	1207.2	Caryophylliidae	*Caryophyllia*	*diomedeae*	5.04	14.5	35.9	12958	680	12696	313
JC066	Coral	-41.3560	42.9185	1002	952	Caryophylliidae	*Desmophyllum*	*dianthus*	7.71	24.4	32.5	13045	581	12373	213
JC066	Coral	-41.3339	42.9188	1144	1097.2	Caryophylliidae	*Desmophyllum*	*dianthus*	6.53	25.9	26.2	13046	755	13697	88
JC066	Coral	-41.3485	42.9208	1157	1207.2	Caryophylliidae	*Caryophyllia*	*diomedeae*	2.59	12.7	31.2	13049	696	12832	250
JC066	Coral	-41.3339	42.9188	0107	1097.2	Caryophylliidae	*Caryophyllia*	*diomedeae*	4.04	16.3	31.3	13238	635	12967	218

JC066	Coral	-41.3485	42.9208	0135	1207.2	Caryophylliidae	*Caryophyllia*	*diomedeae*	8.36	17.5	34.7	13269	765	12300	275
JC066	Coral	-41.3485	42.9208	1159	1207.2	Flabellidae	*Javania*	*antarctica*	0.46	10.2	20	13319	508		
JC066	Coral	-41.3485	42.9208	0123	1207.2	Caryophylliidae	*Desmophyllum*	*dianthus*	9.24	24.5	31	13364	769	12584	237
JC066	Coral	-41.3485	42.9208	0127	1207.2	Caryophylliidae	*Desmophyllum*	*dianthus*	12	40.3	36.6	13405	752	11450	79
JC066	Coral	-41.3485	42.9208	1061	1207.2	Flabellidae	*Javania*	*antarctica*	0.69	10.7	21.5	13416	689		
JC066	Coral	-41.3485	42.9208	0121	1207.2	Caryophylliidae	*Caryophyllia*	*diomedeae*	31.52	16.4	25	13453	624	12294	163
JC066	Coral	-41.3592	42.9176	1046	*922.5*	Caryophylliidae	*Caryophyllia*	*diomedeae*	2	12.9	23.3	13600	735	12933	202
JC066	Coral	-41.3485	42.9208	1070	1207.2	Caryophylliidae	*Desmophyllum*	*dianthus*	2.02	16.6	25	13747	677	14053	131
JC066	Coral	-41.3485	42.9208	0122	1207.2	Caryophylliidae	*Caryophyllia*	*diomedeae*	7.16	20.7	42.5	13782	633	12537	185
JC066	Coral	-41.3339	42.9188	0486Y	1097.2	Caryophylliidae	*Desmophyllum*	*dianthus*	6.33	21.7	25.9	13908	656		
JC066	Coral	-41.3485	42.9208	1158	1207.2	Caryophylliidae	*Desmophyllum*	*dianthus*	1.32	13.9	18.4	13977	728	12924	183
JC066	Coral	-41.3485	42.9208	1065	1207.2	Caryophylliidae	*Desmophyllum*	*dianthus*	5.75	22.3	28.4	14668	830	12824	93
JC066	Coral	-41.3592	42.9176	1045	*922.5*	Caryophylliidae	*Desmophyllum*	*dianthus*	1.71	13.4	17.2	15893	706	12786	125
JC066	Coral	-41.3339	42.9188	1143B	1097.2	Caryophylliidae	*Desmophyllum*	*dianthus*	8.8	3.5	4	16417	709	16492	431
JC066	Coral	-41.3339	42.9188	0486E	1097.2	Caryophylliidae	*Desmophyllum*	*dianthus*	0.8	12.4	25.4	16892	905		
JC066	Coral	-41.3592	42.9176	1040	*922.5*	Caryophylliidae	*Desmophyllum*	*dianthus*	4.73	21.9	26.7	17406	756	16310	253
JC066	Coral	-41.3339	42.9188	1143A	1097.2	Caryophylliidae	*Desmophyllum*	*dianthus*	14.81	40	45.5	17666	801	16447	295
JC066	Coral	-41.3485	42.9208	0115	1207.2	Caryophylliidae	*Desmophyllum*	*dianthus*	2.96	19.7	23.3	24190	2176		
JC066	Coral	-41.3485	42.9208	1058	1207.2	Flabellidae	*Javania*	*antarctica*	0.69	14.9	18.7				
JC066	Coral	-41.3485	42.9208	1060	1207.2	Caryophylliidae	*Desmophyllum*	*dianthus*	0.65	8	29.4				
JC066	Coral	-41.3485	42.9208	1154	1207.2	Dendrophylliidae	*Balanophyllia*	*malouinensis*	0.74	14.2	19.5				
JC066	Coral	-41.3627	42.9151	2797	710	Flabellidae	*Flabellum*	*flexuosum*	0.96	10	27				
JC066	Coral	-41.3628	42.9151	2812	709.5	Dendrophylliidae	*Balanophyllia*	*gigas*	0.15	5	10.1				
JC066	Coral	-41.3339	42.9188	0486B	1097.2	Flabellidae	*Javania*	*antarctica*	0.41	16	18.1				
JC066	Coral	-41.3339	42.9188	0486X	1097.2	Caryophylliidae	*Desmophyllum*	*dianthus*	4.83	fragmentary	3.7			11579	431
JC066	Coral	-41.3485	42.9208	1067B	1207.2	Caryophylliidae	*?*	*?*	0.54	fragmentary	fragmentary				
JC066	Coral	-41.3627	42.9151	2794B	710	Dendrophylliidae	*Balanophyllia*	*gigas*	1.59	0.6	1.5				
JC066	Coral	-41.3628	42.9151	2812H	709.5	Caryophylliidae	*Desmophyllum*	*dianthus*	0.7	10	16.1				
JC066	Coral	-41.3628	42.9151	2812N	709.5	Flabellidae	*Flabellum*	*?*	0.21	8.9	19.1				
JC066	Coral	-41.3628	42.9151	2812O	709.5	Dendrophylliidae	*Leptopsammia*	*stokesiana*	0.12	6	11.7				
JC066	Coral	-41.3628	42.9151	2812P	709.5	Dendrophylliidae	*Balanophyllia*	*gigas*	0.3	6.4	14.2				

JC066	Coral	-41.3628	42.9151	2812S	709.5	Dendrophylliidae	*Balanophyllia*	*gigas*	0.14	4.7	13.7				
JC066	Coral	-41.3628	42.9151	2812T	709.5	Dendrophylliidae	*Balanophyllia*	*gigas*	0.17	5.8	11.1				
JC066	Coral	-41.3628	42.9151	2812U	709.5	Dendrophylliidae	*Balanophyllia*	*gigas*	0.24	7.2	14.8				
JC066	Coral	-41.3628	42.9151	2812W	709.5	Dendrophylliidae	*Balanophyllia*	*gigas*	0.11	4.9	9.8				
JC066	Melville	-38.4741	46.7461	3245	171.9	Caryophylliidae	*Caryophyllia*	*profunda*	27.18	30.6	46.6	841	1585	121	19
JC066	Melville	-38.4983	46.7234	2823	897	Caryophylliidae	*?*	*?*	1.02	12.7	23	6561	539		
JC066	Melville	-38.4983	46.7234	3138J	897	Caryophylliidae	*?*	*?*	0.3	1	1.4	15547	734		
JC066	Melville	-38.4983	46.7234	2825	897	Caryophylliidae	*Caryophyllia*	*?*	4.32	14.2	24	18412	931	16670	343
JC066	Melville	-38.4983	46.7234	3138M	897	Flabellidae	*Flabellum*	*?*	2.1	20.3	22.3	142608	7844		
JC066	Melville	-38.4983	46.7234	2822	897	Caryophylliidae	*Desmophyllum*	*dianthus*	0.17	7.5	9.2				
JC066	Melville	-38.4983	46.7234	2824	897	Dendrophylliidae	*Balanophyllia*	*malouinensis*	1.88	1.1	2.1				
JC066	Melville	-38.4983	46.7234	3138B	897	Deltocyathidae	*Deltocyathus*	*deltocyathus*	0.06	0.5	0.2				
JC066	Melville	-38.4983	46.7234	3138D	897	Flabellidae	*Javania*	*antarctica*	0.18	7.7	13				
JC066	MoW	-37.9567	50.4074	3507	1014	Caryophylliidae	*Caryophyllia*	*diomedeae*	2.9	16	26.4	9435	594	9874	204
JC066	MoW	-37.9567	50.4074	3508	1014	Caryophylliidae	*Caryophyllia*	*diomedeae*	4.92	15.2	29.2	12396	695	12492	117
JC066	MoW	-37.9567	50.4074	3509	1014	Caryophylliidae	*Caryophyllia*	*diomedeae*	4.58	16.5	30	13555	832	12574	297
JC066	MoW	-37.9567	50.4074	3506B	1014	Caryophylliidae	*?*	*?*	2.8	1	2.6	14157	2084	15686	584
JC066	MoW	-37.9567	50.4074	3506A	1014	Caryophylliidae	*Caryophyllia*	*diomedeae*	2.8	14.1	24.1	15863	2063	15562	506
JC066	MoW	-37.9567	50.4074	2590	1014	Caryophylliidae	*Caryophyllia*	*diomedeae*	10	12.9	32	16060	596	15038	271
JC066	MoW	-37.9567	50.4074	3510	1014	Caryophylliidae	*Caryophyllia*	*diomedeae*	7.53	21.6	35.4	17557	866	16066	368
JC066	Atlantis	-32.7223	57.2483	2619	922	Caryophylliidae	*Caryophyllia*	*diomedeae*	3.22	18.3	23.5	0	318		
JC066	Atlantis	-32.7166	57.2451	3718	1035	Caryophylliidae	*Desmophyllum*	*dianthus*	4.42	21.7	23.5	166	201	53	7
JC066	Atlantis	-32.7222	57.2529	3697	823	Caryophylliidae	*Caryophyllia*	*diomedeae*	9.81	18.8	25	200	127	105	19
JC066	Atlantis	-32.7166	57.2451	3692	1035	Caryophylliidae	*Desmophyllum*	*dianthus*	4.12	14.7	16.1	304	133		
JC066	Atlantis	-32.6987	57.2945	3770	763	Caryophylliidae	*Caryophyllia*	*diomedeae*	2.25	15	15.9	344	221		
JC066	Atlantis	-32.7225	57.2500	3721	870	Caryophylliidae	*Desmophyllum*	*dianthus*	0.48	10.9	12.7	348	158		
JC066	Atlantis	-32.7223	57.2483	2621	922	Caryophylliidae	*Caryophyllia*	*diomedeae*	1.77	12.5	22.5	360	155		
JC066	Atlantis	-32.7166	57.2451	3715	1035	Caryophylliidae	*Desmophyllum*	*dianthus*	3.68	16.7	23.9	376	116		
JC066	Atlantis	-32.6987	57.2945	3741	763	Caryophylliidae	*Caryophyllia*	*diomedeae*	3.14	15.9	20.5	413	146	171	26
JC066	Atlantis	-32.7223	57.2483	2618	922	Caryophylliidae	*Caryophyllia*	*diomedeae*	6.02	16	31.9	541	233		
JC066	Atlantis	-32.7122	57.2833	3643	726	Caryophylliidae	*Caryophyllia*	*diomedeae*	8.43	22.4	22.7	582	153	296	43

JC066	Atlantis	-32.7223	57.2483	2617	922	Caryophylliidae	*Caryophyllia*	*diomedeae*	2.23	12.2	30.2	607	184		
JC066	Atlantis	-32.7117	57.2758	3661	743	Caryophylliidae	*Caryophyllia*	*diomedeae*	4.45	15.7	30.5	762	212		
JC066	Atlantis	-32.7223	57.2483	2620	922	Caryophylliidae	*Caryophyllia*	*diomedeae*	3.08	16.5	18.7	845	249	396	26
JC066	Atlantis	-32.7225	57.2500	3705	870	Caryophylliidae	*Caryophyllia*	*diomedeae*	9.25	20.1	30.2	965	187	562	81
JC066	Atlantis	-32.7225	57.2500	3712	870	Caryophylliidae	*Caryophyllia*	*diomedeae*	14.52	18.4	25.3	1435	263	926	11
JC066	Atlantis	-32.7222	57.2529	3696	823	Caryophylliidae	*Caryophyllia*	*diomedeae*	5.27	17	36	2209	397	1994	47

*Italics indicate depth estimated from incomplete cruise record

Appendix 2: Laser ablation U-series dating of SWIO CWCs.

Sample number (JC066_)	LA ID	LA Age / y	2σ	^{238}U (V)	2σ	^{230}Th (V)	2σ	measured $^{230}Th/^{238}U$	2σ	corrected [$^{230}Th/^{238}U$]	2σ
0121	In-001	**13453**	**624**	0.2719	0.0080	3.39E-07	1.73E-08	1.24E-06	4.54E-08	0.1325	0.0056
2812B	In-002	**166**	**147**	0.2599	0.0093	1.54E-08	2.81E-09	5.89E-08	1.07E-08	0.0017	0.0015
0123	In-003	**13364**	**769**	0.1720	0.0036	2.17E-07	1.08E-08	1.26E-06	5.81E-08	0.1317	0.0070
2810	In-004	**327**	**277**	0.1375	0.0027	1.30E-08	2.45E-09	9.49E-08	1.80E-08	0.0034	0.0029
2812G	In-005	**329**	**155**	0.2666	0.0071	1.70E-08	2.89E-09	6.40E-08	1.08E-08	0.0034	0.0016
2799B	In-006	**1957**	**245**	0.2467	0.0068	5.43E-08	5.01E-09	2.20E-07	2.02E-08	0.0203	0.0025
2812C	In-007	**1571**	**243**	0.1998	0.0050	3.85E-08	3.92E-09	1.94E-07	2.05E-08	0.0164	0.0025
3696	In-008	**2209**	**397**	0.1079	0.0025	3.12E-08	3.35E-09	2.88E-07	2.97E-08	0.0229	0.0041
3509	In-009	**13555**	**832**	0.1425	0.0056	1.84E-07	9.97E-09	1.30E-06	6.27E-08	0.1335	0.0075
1040	In-010	**17406**	**756**	0.1877	0.0094	3.08E-07	1.53E-08	1.65E-06	5.36E-08	0.1683	0.0065
1144	In-013	**13046**	**755**	0.1413	0.0035	1.82E-07	9.88E-09	1.29E-06	6.11E-08	0.1287	0.0069
1066B	In-014	**12818**	**792**	0.1411	0.0030	1.79E-07	1.01E-08	1.27E-06	6.31E-08	0.1266	0.0072
2618	In-015	**541**	**233**	0.1312	0.0031	1.55E-08	2.39E-09	1.18E-07	1.79E-08	0.0057	0.0024
2795	In-016	**609**	**227**	0.1454	0.0041	1.74E-08	2.52E-09	1.20E-07	1.73E-08	0.0064	0.0024
1056	In-017	**12339**	**615**	0.1789	0.0042	2.19E-07	1.02E-08	1.22E-06	5.00E-08	0.1222	0.0056
3507	In-018	**9435**	**594**	0.1292	0.0039	1.26E-07	6.90E-09	9.79E-07	5.03E-08	0.0947	0.0056
3712	In-019	**1435**	**263**	0.1016	0.0026	1.71E-08	2.43E-09	1.70E-07	2.45E-08	0.0150	0.0027
2812J	In-020	**1579**	**175**	0.2011	0.0063	3.41E-08	3.34E-09	1.70E-07	1.67E-08	0.0164	0.0018
2812I	In-021	**1237**	**186**	0.2123	0.0084	2.87E-08	3.86E-09	1.36E-07	1.76E-08	0.0129	0.0019
0127	In-022	**13405**	**752**	0.1420	0.0029	2.24E-07	1.08E-08	1.57E-06	6.55E-08	0.1321	0.0068
1143B	In-023	**16417**	**709**	0.1602	0.0083	2.96E-07	1.61E-08	1.86E-06	5.88E-08	0.1595	0.0061

1143A	In-024	**17666**	**801**	0.1755	0.0025	3.44E-07	1.35E-08	1.96E-06	6.57E-08	0.1706	0.0069
3510	In-025	**17557**	**866**	0.1417	0.0047	2.89E-07	1.52E-08	2.03E-06	7.09E-08	0.1697	0.0075
0117	In-026	**1476**	**280**	0.1455	0.0039	4.50E-08	4.12E-09	3.09E-07	2.60E-08	0.0154	0.0029
2619	In-027	**-498**	**318**	0.0885	0.0027	1.48E-08	1.90E-09	1.68E-07	2.15E-08	-0.0052	-0.0033
0128	In-028	**12053**	**1090**	0.0552	0.0016	9.80E-08	5.58E-09	1.78E-06	9.88E-08	0.1195	0.0101
2812D	In-029	**-167**	**362**	0.0939	0.0039	2.00E-08	2.35E-09	2.14E-07	2.44E-08	-0.0018	-0.0038
1145	In-030	**10670**	**1010**	0.0670	0.0031	1.04E-07	6.36E-09	1.58E-06	1.02E-07	0.1065	0.0095
0157	In-031	**9777**	**1419**	0.0329	0.0022	5.57E-08	4.97E-09	1.72E-06	1.27E-07	0.0979	0.0135
3506B	In-032	**14157**	**2084**	0.0251	0.0015	5.89E-08	4.84E-09	2.39E-06	2.17E-07	0.1390	0.0191
3506A	In-033	**15863**	**2063**	0.0282	0.0006	6.90E-08	5.44E-09	2.45E-06	1.95E-07	0.1545	0.0186
3245	In-034	**841**	**1585**	0.0209	0.0007	1.68E-08	2.73E-09	8.15E-07	1.35E-07	0.0088	0.0165
2812L	In-035	**1072**	**1291**	0.0302	0.0016	1.85E-08	3.60E-09	6.37E-07	1.29E-07	0.0112	0.0134
2809	In-036	**2796**	**1474**	0.0241	0.0008	2.26E-08	3.04E-09	9.41E-07	1.24E-07	0.0289	0.0151
2620	In-037	**845**	**249**	0.1392	0.0034	2.63E-08	3.44E-09	1.89E-07	2.36E-08	0.0088	0.0026
3508	In-038	**12396**	**695**	0.1515	0.0032	2.08E-07	9.60E-09	1.38E-06	6.21E-08	0.1227	0.0064
1057	In-039	**154**	**111**	0.2444	0.0126	1.76E-08	2.48E-09	7.35E-08	1.01E-08	0.0016	0.0012
2812R	In-040	**12395**	**522**	0.2307	0.0076	2.99E-07	1.32E-08	1.30E-06	4.54E-08	0.1227	0.0047
2812V	In-041	**1689**	**176**	0.2678	0.0086	5.86E-08	5.37E-09	2.16E-07	1.63E-08	0.0176	0.0018
0124	In-042	**12050**	**709**	0.1257	0.0033	1.64E-07	9.21E-09	1.30E-06	6.07E-08	0.1195	0.0065
1064	In-043	**12268**	**592**	0.2382	0.0053	3.00E-07	1.38E-08	1.26E-06	5.04E-08	0.1215	0.0054
2812K	In-044	**460**	**115**	0.2390	0.0098	1.61E-08	2.72E-09	6.67E-08	1.10E-08	0.0048	0.0012
2812E	In-045	**471**	**113**	0.2705	0.0095	1.79E-08	3.04E-09	6.61E-08	1.10E-08	0.0049	0.0012
2808	In-046	**369**	**147**	0.2821	0.0116	2.07E-08	3.74E-09	7.31E-08	1.33E-08	0.0039	0.0015
2812Q	In-047	**511**	**173**	0.2274	0.0088	2.20E-08	3.46E-09	9.66E-08	1.54E-08	0.0054	0.0018
2799	In-048	**567**	**171**	0.2297	0.0101	2.34E-08	3.40E-09	1.03E-07	1.48E-08	0.0059	0.0018

1116	In-049	**4058**	**410**	0.1486	0.0029	7.42E-08	5.53E-09	5.02E-07	3.92E-08	0.0418	0.0041
2803	In-050	**473**	**133**	0.2319	0.0059	2.30E-08	2.55E-09	9.96E-08	1.12E-08	0.0050	0.0014
2807	In-050	**474**	**133**	0.2319	0.0059	2.30E-08	2.55E-09	9.96E-08	1.12E-08	0.0050	0.0014
2812M	In-051	**1332**	**138**	0.2899	0.0074	5.44E-08	4.26E-09	1.87E-07	1.32E-08	0.0139	0.0014
0107	In-052	**1314**	**139**	0.3359	0.0121	6.05E-08	4.56E-09	1.83E-07	1.51E-08	0.0137	0.0014
1002	In-053	**13238**	**635**	0.1922	0.0119	2.77E-07	1.62E-08	1.45E-06	5.78E-08	0.1305	0.0057
1065	In-054	**13045**	**581**	0.2480	0.0050	3.64E-07	1.44E-08	1.47E-06	4.87E-08	0.1287	0.0052
0119	In-055	**14668**	**830**	0.1998	0.0029	3.29E-07	1.53E-08	1.65E-06	7.43E-08	0.1436	0.0074
2823	In-057	**73510**	**3021**	0.2453	0.0040	1.55E-06	3.12E-08	6.32E-06	1.21E-07	0.5537	0.0148
0120	In-058	**6561**	**539**	0.1395	0.0065	1.15E-07	9.36E-09	8.24E-07	5.64E-08	0.0667	0.0053
1069	In-059	**12418**	**622**	0.2060	0.0049	2.96E-07	1.42E-08	1.44E-06	5.75E-08	0.1229	0.0056
0486C	In-060	**10911**	**613**	0.1429	0.0114	1.97E-07	1.56E-08	1.39E-06	5.79E-08	0.1088	0.0057
1058	In-061	**6610**	**809**	0.0690	0.0024	7.04E-08	5.70E-09	1.03E-06	7.95E-08	0.0672	0.0080
3138J	In-063	**15547**	**734**	0.1673	0.0024	2.49E-07	9.39E-09	1.49E-06	5.63E-08	0.1516	0.0065
1061	In-064	**13416**	**689**	0.3066	0.0047	3.91E-07	1.80E-08	1.27E-06	5.36E-08	0.1322	0.0062
1104A	In-065	**5193**	**389**	0.1927	0.0057	1.07E-07	6.91E-09	5.55E-07	3.43E-08	0.0532	0.0038
1104B	In-066	**5013**	**326**	0.2161	0.0069	1.09E-07	6.23E-09	5.05E-07	2.75E-08	0.0514	0.0032
0486D	In-067	**12289**	**600**	0.3077	0.0050	3.51E-07	1.34E-08	1.15E-06	4.58E-08	0.1217	0.0055
1070	In-068	**13747**	**677**	0.2139	0.0032	2.73E-07	1.15E-08	1.28E-06	5.14E-08	0.1352	0.0061
0115	In-069	**24190**	**2176**	0.1832	0.0043	3.81E-07	2.96E-08	2.09E-06	1.56E-07	0.2267	0.0180
2811	In-070	**553**	**134**	0.2729	0.0081	1.86E-08	2.80E-09	6.92E-08	1.07E-08	0.0058	0.0014
0486Y	In-071	**13908**	**656**	0.1903	0.0047	2.40E-07	9.83E-09	1.27E-06	4.74E-08	0.1367	0.0059
1159	In-072	**13319**	**508**	0.3751	0.0063	4.50E-07	1.45E-08	1.20E-06	3.49E-08	0.1313	0.0045
3138M	In-073	**142608**	**7844**	0.2700	0.0137	2.00E-06	9.73E-08	7.42E-06	1.19E-07	0.8128	0.0194
1062	In-074	**6832**	**333**	0.2991	0.0083	1.91E-07	9.54E-09	6.39E-07	2.65E-08	0.0694	0.0032

1158	In-075	**13977**	**728**	0.2116	0.0049	2.72E-07	1.24E-08	1.29E-06	5.61E-08	0.1373	0.0066
3770	In-076	**344**	**221**	0.1540	0.0049	9.20E-09	2.65E-09	5.91E-08	1.68E-08	0.0036	0.0023
2812F	In-077	**527**	**208**	0.1544	0.0038	1.19E-08	2.40E-09	7.67E-08	1.49E-08	0.0055	0.0022
1059	In-078	**12744**	**607**	0.1764	0.0033	2.12E-07	8.84E-09	1.21E-06	4.84E-08	0.1259	0.0055
2825	In-079	**18412**	**931**	0.1311	0.0042	2.22E-07	8.68E-09	1.70E-06	6.66E-08	0.1772	0.0080
3721	In-080	**348**	**158**	0.1342	0.0033	6.45E-09	1.66E-09	4.78E-08	1.22E-08	0.0036	0.0016
3741	In-081	**413**	**146**	0.1238	0.0019	5.46E-09	1.66E-09	4.36E-08	1.32E-08	0.0043	0.0015
0126B	In-082	**12930**	**649**	0.1834	0.0045	2.27E-07	1.26E-08	1.23E-06	5.28E-08	0.1277	0.0059
1072	In-083	**12762**	**665**	0.1375	0.0062	1.68E-07	9.92E-09	1.23E-06	5.58E-08	0.1261	0.0060
1157	In-084	**13049**	**696**	0.1711	0.0060	2.17E-07	1.30E-08	1.26E-06	5.80E-08	0.1288	0.0063
1045	In-085	**15893**	**706**	0.1389	0.0053	2.11E-07	1.14E-08	1.52E-06	5.57E-08	0.1548	0.0062
1063	In-086	**7176**	**491**	0.1438	0.0059	1.04E-07	5.80E-09	7.31E-07	4.44E-08	0.0728	0.0048
3661	In-087	**762**	**212**	0.1126	0.0033	9.43E-09	2.26E-09	8.29E-08	1.90E-08	0.0080	0.0022
486E	In-088	**16892**	**905**	0.1093	0.0032	1.77E-07	9.82E-09	1.62E-06	7.22E-08	0.1637	0.0079
2617	In-089	**607**	**184**	0.0993	0.0034	6.79E-09	1.55E-09	6.81E-08	1.56E-08	0.0063	0.0019
1160	In-090	**12635**	**789**	0.1356	0.0031	1.68E-07	1.01E-08	1.24E-06	6.87E-08	0.1249	0.0072
3643	In-091	**582**	**153**	0.1162	0.0115	7.29E-09	1.86E-09	6.41E-08	1.66E-08	0.0061	0.0016
3692	In-092	**304**	**133**	0.1132	0.0030	3.86E-09	1.46E-09	3.41E-08	1.31E-08	0.0032	0.0014
0125	In-093	**11975**	**705**	0.1280	0.0044	1.50E-07	1.01E-08	1.17E-06	5.92E-08	0.1188	0.0065
3718	In-094	**166**	**201**	0.1032	0.0027	3.84E-09	1.63E-09	3.72E-08	1.59E-08	0.0017	0.0021
2621	In-095	**360**	**155**	0.1164	0.0065	6.37E-09	1.15E-09	5.43E-08	9.76E-09	0.0038	0.0016
1156	In-096	**10521**	**727**	0.1214	0.0023	1.25E-07	7.99E-09	1.03E-06	6.22E-08	0.1051	0.0068
0135	In-097	**13269**	**765**	0.1533	0.0065	1.96E-07	1.28E-08	1.28E-06	6.31E-08	0.1308	0.0069
3715	In-098	**376**	**116**	0.1528	0.0059	6.19E-09	1.64E-09	4.05E-08	1.07E-08	0.0039	0.0012
1155	In-099	**12767**	**629**	0.1390	0.0036	1.70E-07	7.99E-09	1.23E-06	5.13E-08	0.1262	0.0057

0122	In-100	**13782**	**633**	0.1952	0.0050	2.57E-07	1.20E-08	1.32E-06	5.04E-08	0.1355	0.0057
0118	In-101	**12958**	**680**	0.1393	0.0091	1.73E-07	1.60E-08	1.23E-06	5.57E-08	0.1279	0.0062
1046	In-102	**13600**	**735**	0.1603	0.0048	2.14E-07	1.21E-08	1.33E-06	6.19E-08	0.1338	0.0066
3705	In-103	**965**	**187**	0.1519	0.0076	1.67E-08	2.85E-09	1.08E-07	1.72E-08	0.0101	0.0019
3697	In-104	**200**	**127**	0.1676	0.0051	4.96E-09	1.76E-09	2.94E-08	1.02E-08	0.0021	0.0013
2590	In-105	**16060**	**596**	0.1405	0.0067	2.26E-07	1.28E-08	1.61E-06	4.29E-08	0.1563	0.0051

Measured $^{230}Th/^{238}U$ ratio was corrected for fractionation using a bracketing standard and converted to ages by iteratively solving the decay equation.

Appendix 3: Isotope dilution U-series dating of SWIO CWCs.

Sample number (JC066_)	Age after ini. ^{230}Th corr. / y	2 σ	Age before ini. ^{230}Th corr. / y	2 σ	$\delta^{234}U_m$	2 σ	$\delta^{234}U_i$	2 σ	^{238}U / ppm	2 σ	^{232}Th / ppt	2 σ	[^{230}Th/^{238}U] analytical	2 σ
3718	53	7	60	2	146.9	1.0	146.9	1.0	3.36	0.01	50	0.36	0.0006	1.94E-05
2810	99	17	116	2	146.9	1.0	146.9	1.0	3.42	0.01	124	0.57	0.0012	1.57E-05
3697	105	19	124	2	147.4	1.0	147.4	1.0	3.57	0.01	143	0.72	0.0013	1.87E-05
3245	121	19	140	2	146.9	1.1	146.9	1.1	4.18	0.01	169	0.72	0.0015	1.80E-05
3741	171	26	198	2	146.2	1.0	146.3	1.0	3.21	0.01	184	0.79	0.0021	2.25E-05
3643	296	43	338	4	146.3	1.1	146.4	1.1	3.63	0.01	335	1.47	0.0035	4.36E-05
2620	396	26	421	4	146.9	1.1	147.0	1.1	3.45	0.01	190	0.84	0.0044	3.77E-05
2795	486	128	614	4	146.4	1.0	146.6	1.0	3.84	0.01	1066	4.34	0.0064	4.37E-05
3705	562	81	644	4	146.3	1.0	146.5	1.0	3.14	0.01	554	2.24	0.0067	4.31E-05
3712	926	11	934	6	146.4	1.0	146.8	1.0	3.15	0.01	58	0.33	0.0098	6.64E-05
0117	1782	48	1829	10	146.5	1.1	147.2	1.1	4.64	0.01	473	1.96	0.0191	9.65E-05
3696	1994	47	2040	11	146.0	1.1	146.8	1.1	3.35	0.01	332	1.44	0.0212	1.12E-04
1116	3790	352	4141	21	146.4	1.0	148.0	1.0	4.06	0.01	3088	12.54	0.0427	2.08E-04
3507	9874	204	10064	77	143.0	2.4	147.0	2.5	3.69	0.02	1517	6.29	0.1008	7.03E-04
1156	10568	290	10853	56	145.2	1.0	149.6	1.1	3.76	0.01	2324	9.60	0.1086	5.24E-04
0157	11262	242	11496	57	143.8	1.1	148.5	1.1	3.73	0.01	1895	7.74	0.1145	5.30E-04
0127	11450	79	11468	77	145.1	1.1	149.9	1.1	3.65	0.01	55	0.32	0.1144	7.29E-04
0486x	11579	431	12003	78	147.4	1.2	152.3	1.2	3.51	0.01	1294	5.23	0.1197	7.25E-04
0124	11941	320	12253	76	146.7	1.1	151.7	1.1	3.97	0.01	1071	4.33	0.1220	7.07E-04
0124dup	12097	136	12216	65	145.5	1.0	150.6	1.0	4.49	0.01	1169	4.79	0.1215	6.02E-04
0121	12294	163	12436	82	145.1	1.1	150.2	1.2	4.37	0.01	539	2.22	0.1235	7.58E-04
0135	12300	275	12564	74	143.3	1.2	148.3	1.2	3.71	0.01	851	3.48	0.1245	6.76E-04
1056	12307	985	13285	90	143.0	1.2	148.1	1.3	4.50	0.01	3806	15.33	0.1312	8.26E-04
1002	12373	213	12568	86	144.7	1.1	149.8	1.2	4.21	0.01	715	2.94	0.1247	7.92E-04

1155	12435	134	12554	62	146.5	1.1	151.8	1.1	3.74	0.01	963	3.92	0.1248	5.69E-04
0125	12490	168	12647	63	145.6	1.1	150.8	1.1	3.85	0.01	1306	5.39	0.1256	5.80E-04
3508	12492	117	12572	87	144.0	1.2	149.1	1.2	3.46	0.01	238	1.03	0.1247	8.02E-04
0122	12537	185	12699	89	145.6	1.1	150.9	1.2	4.30	0.01	605	2.51	0.1261	8.22E-04
3509	12574	297	12861	76	145.6	1.1	150.8	1.2	3.83	0.01	959	3.95	0.1276	7.01E-04
0123	12584	237	12805	87	146.5	1.1	151.8	1.2	3.48	0.01	668	2.76	0.1272	8.03E-04
0118	12696	313	13003	63	144.9	1.0	150.2	1.1	4.96	0.01	3316	13.51	0.1288	5.82E-04
0126b	12702	218	12907	73	142.9	1.6	148.1	1.7	4.13	0.01	1836	7.46	0.1277	6.56E-04
1045	12786	125	12894	64	151.9	1.1	157.5	1.1	3.88	0.01	914	3.79	0.1286	5.90E-04
1065	12824	93	12880	75	144.0	1.2	149.4	1.2	4.50	0.01	219	1.00	0.1276	6.83E-04
1157	12832	250	13073	66	143.9	1.1	149.2	1.1	4.86	0.01	2547	10.27	0.1294	6.02E-04
1158	12924	183	13095	65	146.0	1.0	151.5	1.1	4.69	0.01	1742	7.06	0.1298	5.92E-04
1046	12933	202	13125	65	144.7	1.1	150.1	1.1	4.26	0.01	1771	7.18	0.1299	5.96E-04
1066b	12939	185	13101	90	148.8	1.1	154.4	1.1	3.68	0.01	523	2.20	0.1302	8.26E-04
0128	12967	68	12991	63	147.1	1.0	152.6	1.0	4.22	0.01	220	0.94	0.1290	5.83E-04
0107	12967	218	13175	66	147.7	1.1	153.2	1.2	4.03	0.01	1824	7.45	0.1307	6.07E-04
1065dup	12971	81	13018	67	143.7	1.0	149.1	1.1	5.18	0.01	519	2.15	0.1288	6.12E-04
1160	13195	82	13244	65	143.5	1.1	149.0	1.1	4.94	0.01	525	2.20	0.1309	5.97E-04
1144	13697	88	13755	67	144.6	1.0	150.3	1.1	3.54	0.01	441	1.83	0.1358	6.14E-04
1070	14053	131	14163	70	147.9	1.0	153.9	1.0	4.30	0.01	1034	4.23	0.1400	6.43E-04
2590	15038	271	15290	99	141.8	1.1	148.0	1.1	3.70	0.01	808	3.37	0.1496	8.97E-04
3506a	15562	506	16057	99	143.5	1.1	150.0	1.2	3.58	0.01	1530	6.27	0.1568	8.92E-04
3506b	15686	584	16258	113	142.8	1.1	149.3	1.1	4.09	0.01	2033	8.29	0.1585	1.02E-03
3510	16066	368	16418	110	142.9	1.1	149.5	1.1	3.90	0.01	1192	4.87	0.1600	9.77E-04
1040	16310	253	16536	117	143.9	1.1	150.7	1.2	3.92	0.01	768	3.10	0.1612	1.05E-03
1143a	16447	295	16721	104	140.5	1.1	147.2	1.2	3.97	0.01	945	3.86	0.1624	9.25E-04
1143b	16492	431	16911	102	143.6	1.1	150.4	1.2	4.09	0.01	1487	6.09	0.1646	9.03E-04
2825	16670	343	17002	86	138.5	1.1	145.2	1.2	4.58	0.01	3281	13.27	0.1646	7.53E-04

The value $\delta^{234}U_m$ is the present-day deviation (‰) from secular equilibrium of the $^{234}U/^{238}U$ activity ratio in the sample. $\delta^{234}U_i$ is the deviation at the time of carbonate formation, used to test for closed-system behaviour of the corals.

Appendix 4: CWC preservation

Examples of CWC coating and aragonite preservation.

	'High' aragonite preservation	'Low' aragonite preservation
'Low' coating	 JC066_2811; *D. dianthus* (C: 0; A.P: 5)	 JC066_1070*; D. dianthus* (C: 0; A.P: 3; no CWCs in collection were described to have low aragonite preservation and low coating)
'High' coating	 JC066_1056; *C. diomedeae* (C: 3; A.P: 4)	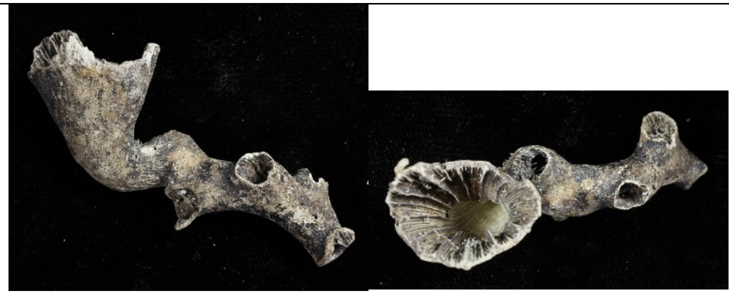 JC066_0115; *D. dianthus* (C: 3; A.P: 1)

The frequency of specimens at each aragonite preservation category (A.P: 1 low, 5 high) at different coating levels (C: 0 low, 3 high).

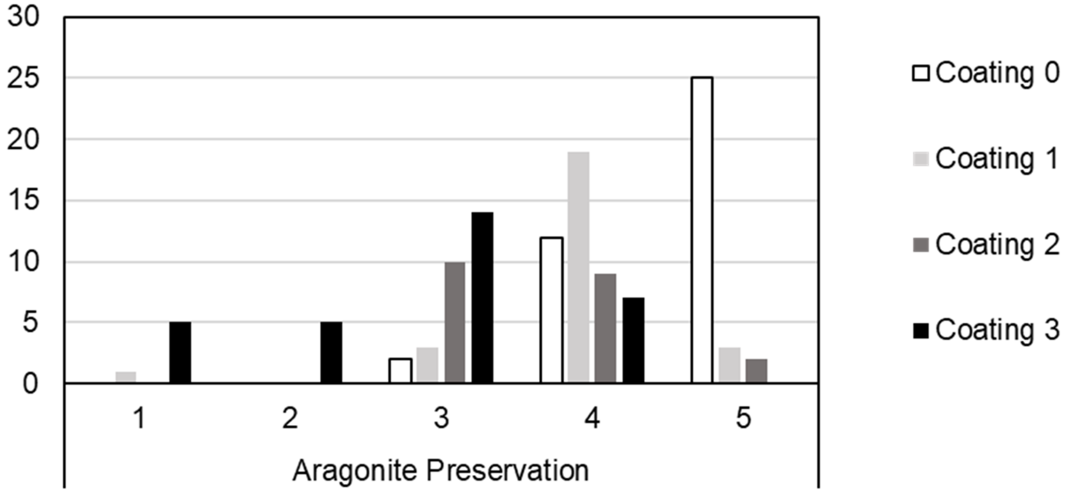

Appendix 5: Additional photographs of cold-water coral specimens: (a) JC066_2812b, *Balanophyllia gigas;* (b) JC066_2812e*, Balanophyllia malouinensis,* (c) JC066_2797, *Flabellum flexuosum;* (d) JC066_1058 *Javania antarctica;* (e) JC066_3245, *Caryophyllia profunda;* (f) JC066_1104a & JC066_1104b, *Trochocyathus gordoni.* All photographs are scaled to the 5mm scale bar except (e) which is scaled to the 10mm scale bar.